A

IB: anti-Myc

	CHX			CHX +MG132		
Treatment (h):	0	1	2	0	1	2
Nuclear						
	1.0	0.3	0.1	0.9	2.7	2.9
Cytosol						
	0.1	0.0	0.0	0.1	1.2	1.0

B

Treatment					
MG132	-	-	-	+	+
CHX	+	+	+	+	+
(h):	0	1.5	3	1.5	3
GATA3					
	1.0	0.2	0.2	1.2	1.0
αTubulin					
	1.0	1.0	1.0	1.0	1.0

C

Treatment				
Lactacystin	-	-	+	-
MG132	-	-	-	+
CHX	+	+	+	+
(h):	0	2	2	2
GATA3				
	1.0	0.2	1.0	1.2
αTubulin				
	1.0	1.0	1.0	0.9

D

	Myc or Flag	TAD		Zinc Finger N C	
WT	#1				#443
dCT	#1				#345
dCF	#1				#315
dZF	#1				#261

E

IB: anti-Myc

	WT			dCT			dCF			dZF		
CHX:	-	+	+	-	+	+	-	+	+	-	+	+
MG132:	-	-	+	-	-	+	-	-	+	-	-	+
Nuclear												
	1.0	0.1	6.6	1.0	0.0	4.2	1.0	0.3	3.0	1.0	0.9	2.1
Cytosol												
	0.1	0.0	2.6	0.7	0.0	3.6	1.5	0.1	2.4	25.1	22.6	27.5

FIG. 4. **GATA3 is rapidly degraded via a 26 S proteasome-dependent pathway.** *A,* GATA3 is degraded in a 26 S proteasome-dependent manner. Myc-tagged GATA3 was introduced into COS cells. The transfected cells were harvested at the indicated time after treatment with cycloheximide (100 μM) and proteasome inhibitor MG132 (50 μM). Nuclear and cytoplasmic extracts were prepared, and the amount of Myc-tagged GATA3 was assessed by immunoblotting *(IB)* with anti-Myc mAb. Arbitrary densitometric units are shown below each band. *B,* splenic CD4 T cells were stimulated under Th2- conditions for 4 days. The cells were then treated with CHX (100 μM) in the presence or absence of MG132 (20 μM) for the indicated times. Total cell extracts were prepared using RIPA lysis buffer. The amount of GATA3 protein was assessed by immunoblotting with anti-GATA3 mAb. Arbitrary densitometric units are shown below each band. *C,* developing Th2 cells prepared as in *B* were treated with CHX (100 μM) in the presence or absence of MG132 (20 μM) or lactacystin (20 μM) for 2 h. The amount of GATA3 protein was assessed as in *B. D,* schematic representation of Myc-tagged GATA3 mutants. Wild type GATA3 *(WT)* and three mutants *(dCT, dCF,* and *dZF)* are shown with the location of the Myc tag *(Myc),* the transactivation domain *(TAD),* and the two zinc finger domains *(N* and *C). E,* degradation and MG132-induced rescue of GATA3 mutants. Myc-tagged GATA3 mutants were transfected into COS7 cells, and the transfectants were treated with the indicated inhibitors for 2 h. The amounts of Myc-tagged GATA3 were assessed as in *A.* Arbitrary densitometric units are shown below each band. Four independent experiments were performed with similar results.

blotting with anti-Ub mAb was performed after anti-FLAG immunoprecipitation (Fig. 5A). Significantly increased levels of multiubiquitination (appears as smear) were observed in the wild type GATA3 transfectants compared with control vector, and the levels were significantly increased in the presence of MG132 (Fig. 5A, compare *lanes 3* and *4*). The levels of multiubiquitination appeared to be equivalent in the case of the dCT mutant (Fig. 5A, *lanes 5* and *6*), slightly decreased in the dCF mutant (*lanes 7* and *8*), and greatly reduced in the dZF mutant (*lanes 9* and *10*). The levels of FLAG-tagged protein in total (nuclear and cytoplasmic) lysates were not reduced in these transfectants (Fig. 5A, *right panel*). Thus, multiubiquitination of GATA3 protein can be readily demonstrated, and it appears that the dZF mutant is the least modified among the mutant forms tested. The multiubiquitination on truncated GATA3 mutants was further assessed by anti-FLAG immunoblotting (Fig. 5B). The levels of multiubiquitination were slightly decreased in the dCF mutant and greatly reduced in the dZF mutant, indicating again that the C-terminal region of GATA3, including the zinc finger region (residues 261–315), is critical for ubiquitination.

We performed an *in vitro* ubiquitination assay as a further demonstration of the multiubiquitination on GATA3. 293T cells were transfected with FLAG-tagged GATA3, and 3 days later, the cells were treated with MG132 for 2 h. *In vitro* ubiquitination was performed after anti-GATA3 immunoprecipitation, and ubiquitinated GATA3 was detected by immunoblotting with anti-GATA3 (Fig. 5C, *left panel*). Concurrently, anti-FLAG immunoprecipitation and anti-FLAG immunoblot-

ting were done (Fig. 5C, *right*). Although variable levels of multiubiquitinated GATA3 were detected without *in vitro* ubiquitination (Fig. 5C, *lane 4*), significantly increased signals with new bands (indicated by *) were detected after *in vitro* ubiquitination (*lane 8*). Similarly, increased ubiquitination was readily detected after *in vitro* ubiquitination in the anti-FLAG immunoblot (Fig. 5C, compare *lanes 12* and *14*).

Next, in order to examine the involvement of activation of the ERK-MAPK cascade in the GATA3 ubiquitination, we assessed the effect of PMA to activate the MAPK cascades and U0126 to inhibit selectively the ERK-MAPK cascade on the ubiquitination of GATA3. 293T cells transfected with FLAG-tagged GATA3 were treated with PMA in the presence or absence of U0126, and then the levels of ubiquitination on GATA3 were assessed (Fig. 5D). Treatment with PMA resulted in a reduction in the degree of ubiquitination of GATA3, and this effect could be reversed significantly by the addition of U0126, suggesting that the ubiquitination of GATA3 is regulated by the activation of ERK MAPK. Similarly, in developing Th2 cells, the ubiquitination of GATA3 protein was detected when the cells were treated with MG132 (20 μM) for 2 h, and the levels in ubiquitination were enhanced in the presence of U0126 (data not shown).

Mdm2 Acts as a Ubiquitin E3 Ligase for GATA3—We wanted to identify possible E3 ligase for GATA3 in developing Th2 cells. Since the association with specific substrates is critical for the function of E3 ligases (32, 45), we first examined the physical association of GATA3 with known E3 ligases that are expressed in lymphocytes (Mdm2, Itch, E6-AP, and Cbl-b).
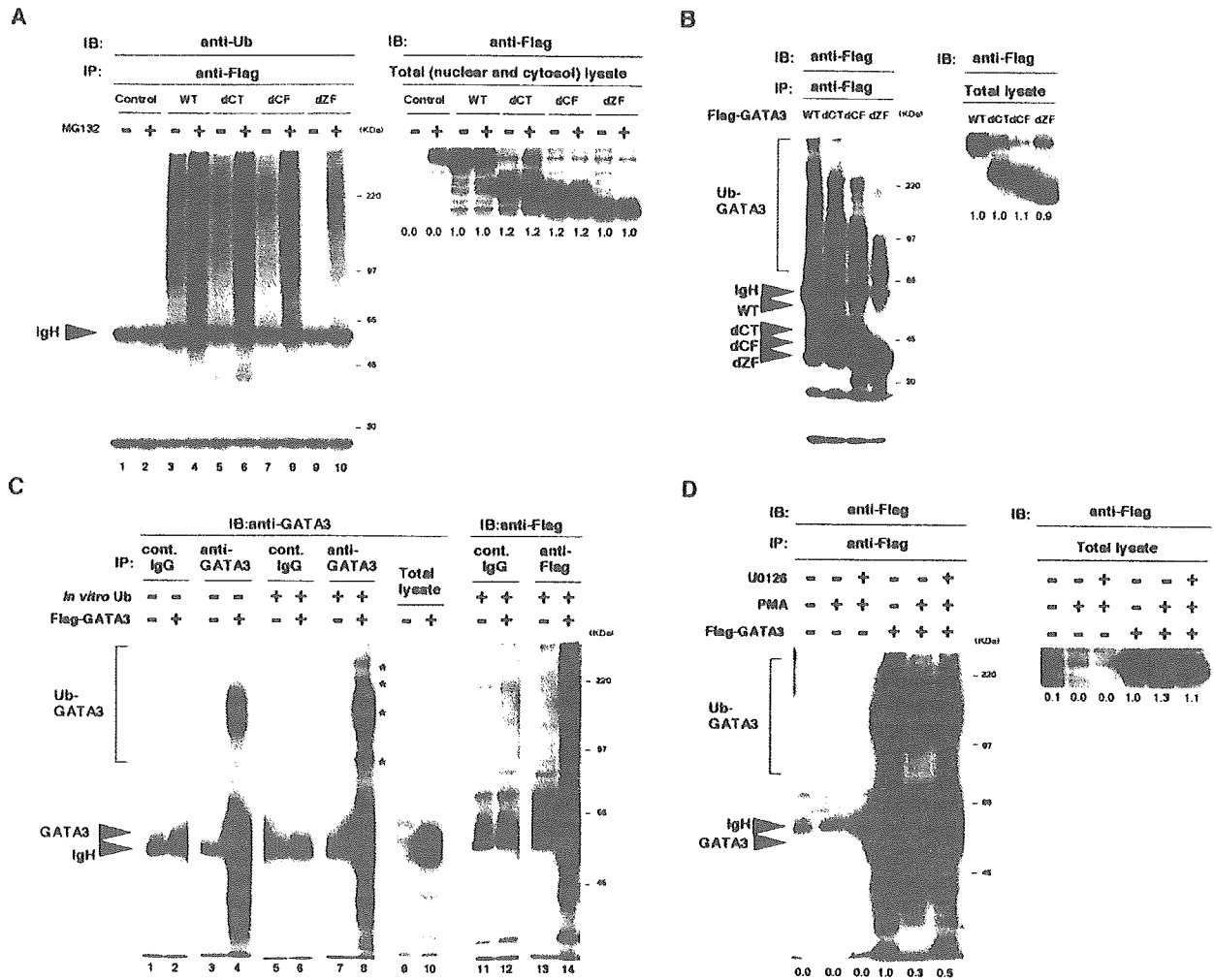
FIG. 5. **GATA3 was ubiquitinated** *in vivo* **and** *in vitro. A,* ubiquitination of GATA3 *in vivo.* 293T cells were transfected with expression plasmids encoding FLAG-tagged GATA3 wild type (*WT*) and mutants (*dCT, dCF,* and *dZF*), and 72 h later were treated with MG132 (50 μM) for 2 h. FLAG-tagged GATA3 was immunoprecipitated (*IP*) with anti-FLAG mAb, and the level of ubiquitination was assessed by immunoblotting (*IB*) with anti-Ub mAb (*left panel*). The levels of FLAG-tagged transfected protein in the total (nuclear and cytoplasmic) lysates were also assessed by anti-FLAG immunoblotting (*right panel*). Arbitrary densitometric units are shown below each lane. *B,* FLAG-tagged GATA3 mutants were immunoprecipitated with anti-FLAG mAb, and the levels of ubiquitination were visualized by immunoblotting with anti-FLAG mAb. The positions of migration of ubiquitinated GATA3 (*Ub-GATA3*), nonubiquitinated GATA3 wild type (*WT*), and mutants (*WT, dCT, dCF,* and *dZF*), and IgH are indicated. Total (nuclear and cytoplasmic) lysates (3 μl) were also run in parallel. Arbitrary densitometric units are shown below each lane. *C,* ubiquitination of GATA3 *in vitro.* 293T cells were transfected with FLAG-tagged GATA3, and 72 h later the cells were treated with MG132 (50 μM) for 2 h. Immunoprecipitates with anti-GATA3 or anti-FLAG mAb were subjected to *in vitro* ubiquitination assay. Ubiquitinated GATA3 was visualized by immunoblotting with anti-GATA3 or anti-FLAG mAb. The positions of migration of ubiquitinated GATA3 (*Ub-GATA3*), nonubiquitinated GATA3 (*GATA3*), and IgH are indicated. The Ub-GATA3 bands that appeared after *in vitro* ubiquitination are indicated by *asterisks.* Total lysates (10 μl) were also run in parallel. *D,* ERK-MAPK cascade controls GATA3 ubiquitination. 293T cells were transfected with FLAG-tagged GATA3. Three days after transfection, the cells were treated with PMA (10 ng/ml) and U0126 (20 μM) for 3 h and then treated with MG132 (50 μM) for 2 h. GATA3 was immunoprecipitated with anti-FLAG mAb and visualized with anti-FLAG immunoblotting. Arbitrary densitometric units of the major Ub-GATA3 band are shown below each lane. Total lysates (3 μl) were also run in parallel.

Freshly isolated splenic CD4 T cells were stimulated with immobilized anti-TCR mAb under Th2– conditions for 3 days in the presence or absence of U0126. Immunoprecipitates with anti-GATA3 mAb were subjected to immunoblotting with anti-Mdm2 mAb and anti-GATA3 mAb (Fig. 6A) and with specific antibodies for several E3 ligases (Fig. 6B). Large amounts of Mdm2 were detected in the GATA3– precipitates from U0126-treated cells, suggesting association of Mdm2 with GATA3, although the amount of GATA3 is significantly reduced (~1/3) in the U0126-treated cells (Fig. 6A). Although there were substantial amounts of E6-AP, Itch, or Cbl-b molecules in developing Th2 cells, no significant quantity of E6-AP, Itch, or Cbl-b was detected in the anti-GATA3 immunoprecipitates under the conditions where substantial amounts of Mdm2 were detected

(Fig. 6B). Thus, the association of Mdm2 with GATA3 appeared to be more selective than that of other E3 ligases (Itch, E6-AP, and Cbl-b).

To characterize further the Mdm2 association with GATA3, 293T cells were transfected with FLAG-tagged GATA3 and their mutants (dCT, dCF, and dZF) and were treated with MG132 for 2 h. Immunoprecipitates with anti-FLAG mAb were immunoblotted with anti-Mdm2 mAb. As shown in Fig. 6B, *upper panel,* association of Mdm2 with GATA3 was readily detected, and the association was apparently decreased in the dCF mutant and almost undetectable in the dZF mutant. The amounts of Mdm2 and FLAG-GATA3 protein in these transfectants were similar (Fig. 6B, *middle* and *bottom panels*). Thus Mdm2 appears to be constitutively associated with wild type
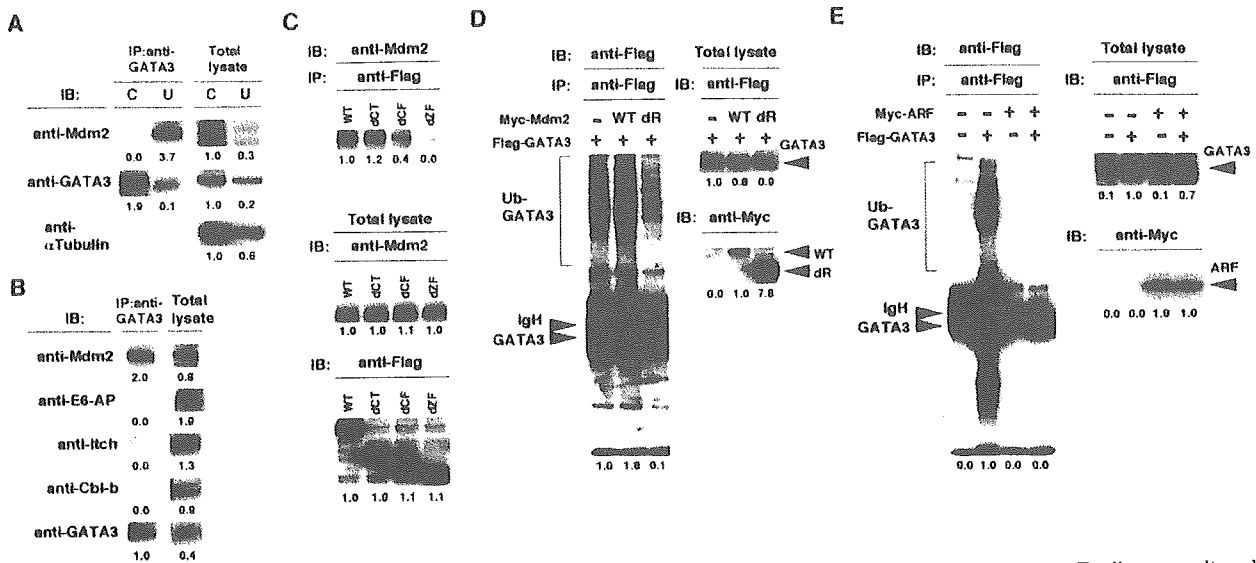
FIG. 6. **Mdm2 acts as an E3 ligase for GATA3.** *A,* Mdm2 is associated with GATA3 in developing Th2 cells. Splenic CD4T cells were cultured under Th2− conditions for 3 days in the presence (*U*) or absence (*C*) of U0126 (20 μM). Immunoprecipitates with anti-GATA3 mAb from the cultured cells were subjected to immunoblotting (*IB*) with anti-Mdm2 and anti-GATA3. Total lysates were also run in parallel. Arbitrary densitometric units are shown below each band. *B,* splenic CD4T cells were cultured under Th2− conditions for 3 days in the presence of U0126 (20 μM). Immunoprecipitates with anti-GATA3 mAb were subjected to immunoblotting with anti-Mdm2, anti-E6-AP, anti-Itch, anti-Cbl-b, and anti-GATA3 antibodies. Total lysates were also run in parallel. Arbitrary densitometric units are shown below each band. *C,* Mdm2 is associated with GATA3 in 293T cells. 293T cells were transfected with FLAG-tagged GATA3 and mutants (*dCT, dCF,* and *dZF*). Three days after transfection, cells were treated with MG132 (50 μM) for 2 h. Immunoprecipitates (*IP*) with anti-FLAG mAb were immunoblotted with anti-Mdm2 mAb. Total lysates (10 μl) were run in parallel. Arbitrary densitometric units of the band are shown below each band. *D,* Mdm2 acts as E3 ligase for GATA3. 293T cells were transfected with FLAG-tagged GATA3 and Myc-tagged wild type (*WT*) Mdm2 or Myc-tagged RING finger-deleted Mdm2. Three days after transfection, cells were treated with MG132 (50 μM) for 2 h. Immunoprecipitates with an anti-FLAG mAb were subjected to immunoblotting with anti-FLAG mAb. Mdm2 was detected by immunoblotting with anti-Myc mAb. The positions of migration of ubiquitinated GATA3 (*Ub-GATA3*), nonubiquitinated GATA3 (*GATA3*), IgH, and Myc-tagged wild type Mdm2 (*WT*) and Myc-tagged RING finger-deleted Mdm2 (*dR*) are indicated. Arbitrary densitometric units of the major Ub-GATA3 band are shown below each lane. *E,* overexpression of ARF suppressed multiubiquitination of GATA3. 293T cells were transfected with FLAG-tagged GATA3 and Myc-tagged ARF. FLAG-tagged GATA3 were immunoprecipitated with anti-FLAG mAb, and the levels of ubiquitination were visualized by immunoblotting with anti-FLAG mAb. Transfected Myc-tagged ARF was detected by immunoblotting with anti-Myc mAb. The positions of migration of ubiquitinated GATA3 (*Ub-GATA3*), nonubiquitinated GATA3 (*GATA3*), IgH and Myc-tagged ARF (*ARF*) are indicated. Arbitrary densitometric units of the major Ub-GATA3 band are shown below each lane.

GATA3 in 293T cells, and the C-terminal region including the zinc finger domain is important for association.

To assess whether Mdm2 has E3 ligase activity for GATA, FLAG-tagged GATA3 and Myc-tagged wild type and a RING finger-deleted Mdm2 were expressed in 293T cells. The RING finger domain of Mdm2 is critical for E3 ligase activity for p53 (46). Immunoprecipitates with an anti-FLAG mAb were subjected to immunoblotting with anti-FLAG mAb. Overexpression of wild type Mdm2 led to increased levels of multiubiquitination of GATA3 (Fig. 6C, *1st two lanes*). More interestingly, the ubiquitination of GATA3 was greatly reduced when the RING finger-deleted Mdm2 was expressed. The levels were much lower than those in cells without Mdm2 transfection, suggesting a dominant-negative feature of the RING finger-deleted Mdm2 to endogenously expressing Mdm2 in 293T cells. The efficiency of expression of the transfected RING finger-deleted Mdm2 was considerably high (Fig. 6C, *right panel*), probably because of the inhibition of ubiquitination itself (47, 48).

It is known that cyclin-dependent kinase inhibitor 2A, a tumor suppressor molecule (p19^{ARF} in the mouse and p14^{ARF} in human cells), binds tightly to Mdm2 and prevents Mdm2-mediated p53 ubiquitination (49). Consequently, we tested the effect of expression of ARF in the GATA3 ubiquitination. As shown in Fig. 6D, *left panel*, the introduction of ARF resulted in nearly complete inhibition of the multiubiquitination of GATA3 in 293T cells. Collectively, these results support the notion that Mdm2 has E3 ligase activity for GATA3.

Mdm2 Is Involved in GATA3 Ubiquitination in T Cells—In order to provide additional evidence to support the role of

Mdm2 as a major E3 ligase, we attempted the inhibition of GATA3 ubiquitination in T cells by using Mdm2 RNA interference. Mdm2 siRNA was introduced in a T cell line TG40 at a high level. The expression levels of Mdm2 protein were reduced significantly upon the introduction of the Mdm2 siRNA as compared with the control (Fig. 7A, *right top panel*). As anticipated, GATA3 ubiquitination was reduced substantially by the Mdm2 siRNA treatment (Fig. 7A, *left panel, lane 1.0 versus 0.4*). These results help to confirm the involvement of Mdm2 in GATA3 ubiquitination in TG40 T cells.

Finally, we wanted to address the function of Mdm2 in primary developing Th2 cells. The mRNA expression of Mdm2 was similar between developing Th1 and Th2 cells (data not shown). Our attempts to silence Mdm2 by RNA interference were unsuccessful with the primary T cells, probably because of robust proliferation of developing Th2 cells in the *in vitro* cultures. Thus we took an alternative approach to inhibit GATA3 ubiquitination and to facilitate Th2 cell differentiation by introducing a RING finger-deleted Mdm2 (Mdm2-dR) into developing Th2 cells (Fig. 7, *B* and *C*). There was substantial expression of endogenous Mdm2 in primary developing Th2 cells, and furthermore, the level of introduced Mdm2-dR by a retrovirus vector was lower than that of endogenous Mdm2 (Fig. 7B, *right top panel*). Nevertheless, GATA3 ubiquitination was significantly reduced (Fig. 7B, *left panel, lane 1.0 versus 0.6*). Moreover, there was significant increase in the generation of IL-4-producing Th2 cells (38.4 *versus* 54.0%) with higher mean fluorescence intensity in IL-4 fluorescence (114.3 *versus* 163.6) when Mdm2-dR was expressed in developing Th2 cells (Fig. 7C). Thus, we conclude that Mdm2 is involved in GATA3
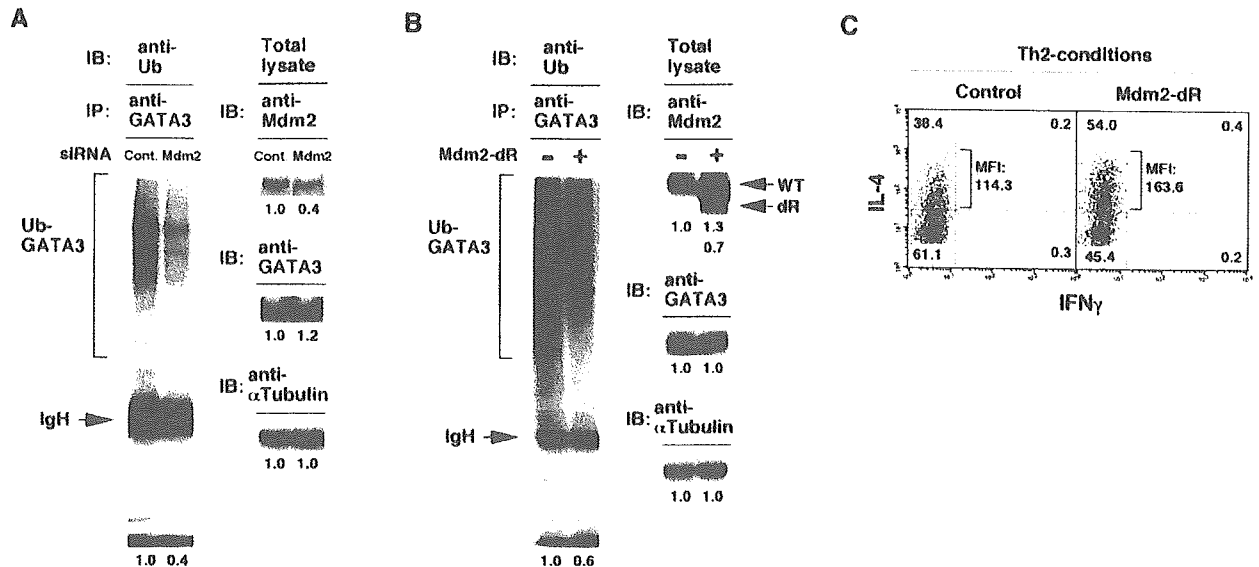
FIG. 7. **Mdm2 is involved in the ubiquitination of GATA3 in T cells.** *A,* inhibition of GATA3 ubiquitination with siRNA for Mdm2. Mouse T cell line TG40 cells were transfected with siRNA specific for Mdm2. Three days after transfection, cells were cultured at 37 °C for 2 h in the presence of MG132 (20 μM). Then the ubiquitination of GATA3 was assessed. Arbitrary densitometric units of the major Ub-GATA3 band are shown below each lane. The expression of Mdm2, GATA3, and α-tubulin is shown on the *right panels. IP,* immunoprecipitation; *IB,* immunoblot. *B,* effect of a dominant-negative (Ring-finger deleted) form of Mdm2 (*Mdm2-dR*) on the ubiquitination of GATA3 in developing Th2 cells. Splenic CD4 T cells were stimulated as described in Fig. 1, and the cells were infected with retrovirus encoding Mdm2 mutant bicistronically with human NGFR. Three days after infection, the NGFR-positive population was enriched by MACS and cultured at 37 °C for 2 h in the presence of MG132 (20 μM). Then the ubiquitination of GATA3 was assessed. Arbitrary densitometric units of the major Ub-GATA3 band are shown below each lane. The expression of Mdm2 (WT and dR), GATA3, and α-tubulin is shown on the *right panels. C,* expression of dominant-negative Mdm2 enhanced Th2 cell development. Freshly prepared splenic CD4 T cells were stimulated under Th2− skewed conditions and infected with retrovirus encoding Mdm2-dR bicistronically with EGFP on day 2. Three days later, the cells were stimulated with anti-TCR and were subjected to cytoplasmic IFNγ/IL-4 staining. Mean fluorescence intensity (*MFI*) of IL-4-staining is also indicated.

ubiquitination in primary Th2 cells and control Th2 cell differentiation.

DISCUSSION

In this paper, we provide evidence indicating that TCR-mediated activation of the Ras-ERK MAPK cascade controls GATA3 protein stability through the ubiquitin-proteasome pathway. The induction of GATA3 protein in developing Th2 cells is crucial for the differentiation of Th2 cells (18, 19). IL-4-induced STAT6 activation initiates transcription of GATA3 (50). However, among the issues that remain to be clarified is how the expression of GATA3 protein is controlled in developing Th2 cells. Here we demonstrate the following. (i) GATA3 protein is very unstable with a short half-life (~1 h) in transfectants (Fig. 4A) and developing Th2 cells (Fig. 4B). (ii) The degradation of GATA3 is dependent on the 26 S proteasome pathway (Fig. 4, A–C). (iii) GATA3 is ubiquitinated both *in vivo* and *in vitro* (Fig. 5). (iv) The deletion of the possible ubiquitination sites of GATA3 led to stable expression of GATA3 and reduced ubiquitination (Fig. 4E and Fig. 5, A and B). From these results, we conclude that the fate of GATA3 in developing Th2 is highly dependent on degradation through the ubiquitin-proteasome system. Concurrently, we show that activation of the ERK-MAPK cascade facilitated GATA3-mediated chromatin remodeling at the Th2 cytokine gene loci (Fig. 1) and inhibited the degradation (Figs. 2 and 3) and ubiquitination of the GATA3 molecule (Fig. 5D). Because the Ras-ERK MAPK cascade in naive CD4 T cells is activated by stimulation of TCR and not of IL-4R (11), the activation of the Ras-ERK MAPK cascade detected in the experiments must be a consequence of TCR-mediated signaling. Therefore, stabilization of GATA3 by the activation of the Ras-ERK MAPK cascade could be the mechanism that accounts for an essential role for TCR-mediated signaling in Th2 cell differentiation.

Our studies identify Mdm2 as a possible E3 ligase for GATA3. Mdm2 was shown to be associated with GATA3 in developing Th2 cells and 293T cells (Fig. 6, A–C). The overexpression of wild type Mdm2 induced increased ubiquitination on GATA3, whereas that of RING finger-deleted mutant Mdm2 resulted in the inhibition of GATA3 ubiquitination in 293T cells (Fig. 6D). Overexpression of ARF, an inhibitor of Mdm2, resulted in almost complete suppression of multiubiquitination of GATA3 in 293T cells (Fig. 6E). Moreover, the introduction of siRNA for Mdm2 into the T cell line TG40 resulted in the reduction in the ubiquitination of GATA3 protein (Fig. 7A). The generation of IL-4-producing Th2 cell was enhanced by the expression of RING finger-deleted mutant Mdm2, suggesting a physiological role for Mdm2 in Th2 cell differentiation (Fig. 7C).

Mdm2 is known to promote degradation of p53 through a ubiquitin-dependent proteasome pathway (49, 51). Mdm2 acts as an E3 ubiquitin ligase specific for p53 *in vitro* (51). The RING finger domain of Mdm2 is critical for E3 ligase activity for p53 (46). The phosphorylation of p53 at serine 15, threonine 18, and serine 20 led to the reduction of Mdm2 binding and enhancement of p53 stabilization and accumulation (49). Most interestingly, amino acid residues 9–20 (SVEPPLSQETFS) of human p53, which are reported to be important for the binding for Mdm2, are highly homologous to amino acid residues 131–142 of human GATA3 (SVYPPASSSSLS) and mouse GATA3 (SVYPPASSSSLA). In these regions, serine/threonine phosphorylation sites and surrounding proline residues (indicated in boldface above) occur in similar patterns between p53 and GATA3. Moreover, GATA3 has other structural similarities with p53, *e.g.* possible lysine ubiquitination sites at the C-terminal region (364–390 in p53 and 396–422 in GATA3) and a proline-rich regulatory region (69–101 in p53 and 146–178 in

GATA3), which are reported to have important roles in post-translational modification and functions of p53 (52, 53). Thus, it is reasonable to expect that a similar set of molecular events operating in ubiquitination of p53 would occur in the case of GATA3

In our experiments with truncation mutants, truncation of the above-mentioned lysine ubiquitination sites in the C-terminal region 396–422 in GATA3 (dCT mutant) resulted in small effects on degradation (Fig. 4E) and multiubiquitination of GATA3 (Fig. 5, A and B). A small but significant effect was observed in the dCF mutant (Fig. 5, A and B). A more prominent effect was observed by deletion of residues 261–443 (dZF mutant) (Fig. 4E and Fig. 5, A and B). The 261–315 region contains three lysine residues (293, 303, and 305 in human GATA3) and a nuclear localization signal (KPKRR). It is known that the degradation of p53 is controlled also by the localization of p53 and Mdm2 (54, 55). Thus, similar to p53, the degradation of GATA3 appears to be controlled by both the ubiquitination process and nuclear/cytosol localization of the protein.

The Ras-ERK MAPK cascade regulates stability of various proteins, including Myc, MKP-1, ATF2, and p53 through a mechanism involving serine phosphorylation (56–61). In addition, ERK MAPK-dependent phosphorylation and the subsequent enhancement of the transcriptional activities for GATA2 and GATA4 have been suggested (62, 63). GATA3 was phosphorylated by activated p38 MAPK in cAMP-treated T cells, suggesting a possible regulatory role for the MAPK cascade in GATA3 function (64). In fact, our preliminary results indicate that an active form of ERK2 directly phosphorylates GATA3 protein *in vitro*, and PMA-induced GATA3 phosphorylation was significantly inhibited by U0126 in transfected COS7 cells.[2] GATA3 protein contains numerous Ser/Thr residues (93 residues out of 444 residues) and possesses 35 putative phosphorylation sites, and thus the precise location of critical amino acid residues responsible for the MAPK-dependent phosphorylation remains unclear at this time. Thus, it appears to be reasonable to surmise that the activation of the ERK-MAPK cascade induces GATA3 phosphorylation and prevents its ubiquitin-mediated degradation through the 26 S proteasome.

Our studies with primary T cells indicated that the ERK-MAPK cascade plays a major role in the regulation of GATA3 protein expression. Although we observed the activation of the p38 MAPK cascade after PMA treatment in developing Th2 cells,[2] a specific inhibitor for the p38 MAPK cascade (SB203580) did not affect the GATA3 protein expression. However, it is still possible that the activation of the p38 MAPK cascade may have some effect on the expression of GATA3 protein as well as the function of GATA3 (64).

In summary, TCR-mediated activation of the Ras-ERK MAPK cascade controls the stability of GATA3 protein by a ubiquitin-proteasome-dependent mechanism. IL-4-induced STAT6 activation is required for the induction of GATA3 transcription. Thus, efficient activation of both signaling pathways and resulting stable GATA3 expression, therefore, are crucial for chromatin remodeling at the Th2 cytokine gene loci and successful Th2 cell differentiation.

REFERENCES

1. Mosmann, T. R., and Coffman, R. L. (1989) *Adv. Immunol.* **46**, 111–147
2. Seder, R. A., and Paul, W. E. (1994) *Annu. Rev. Immunol.* **12**, 635–673
3. Reiner, S. L., and Locksley, R. M. (1995) *Annu. Rev. Immunol.* **13**, 151–177
4. Abbas, A. K., Murphy, K. M., and Sher, A. (1996) *Nature* **383**, 787–793
5. Constant, S. L., and Bottomly, K. (1997) *Annu. Rev. Immunol.* **15**, 297–322
6. O'Garra, A. (1998) *Immunity* **8**, 275–283
7. Gately, M. K., Renzetti, L. M., Magram, J., Stern, A. S., Adorini, L., Gubler, U., and Presky, D. H. (1998) *Annu. Rev. Immunol.* **16**, 495–521
8. Murphy, K. M., Ouyang, W., Farrar, J. D., Yang, J., Ranganath, S., Asnagli, H., Afkarian, M., and Murphy, T. L. (2000) *Annu. Rev. Immunol.* **18**, 451–494
9. Nelms, K., Keegan, A. D., Zamorano, J., Ryan, J. J., and Paul, W. E. (1999) *Annu. Rev. Immunol.* **17**, 701–738
10. Yamashita, M., Hashimoto, K., Kimura, M., Kubo, M., Tada, T., and Nakayama, T. (1998) *Int. Immunol.* **10**, 577–591
11. Yamashita, M., Kimura, M., Kubo, M., Shimizu, C., Tada, T., Perlmutter, R. M., and Nakayama, T. (1999) *Proc. Natl. Acad. Sci. U. S. A.* **96**, 1024–1029
12. Yamashita, M., Katsumata, M., Iwashima, M., Kimura, M., Shimizu, C., Kamata, T., Shin, T., Seki, N., Suzuki, S., Taniguchi, M., and Nakayama, T. (2000) *J. Exp. Med.* **191**, 1869–1879
13. Shibata, Y., Kamata, T., Kimura, M., Yamashita, M., Wang, C. R., Murata, K., Miyazaki, M., Taniguchi, M., Watanabe, N., and Nakayama, T. (2002) *J. Immunol.* **169**, 2134–2140
14. Dong, C., Yang, D. D., Wysk, M., Whitmarsh, A. J., Davis, R. J., and Flavell, R. A. (1998) *Science* **282**, 2092–2095
15. Yang, D. D., Conze, D., Whitmarsh, A. J., Barrett, T., Davis, R. J., Rincon, M., and Flavell, R. A. (1998) *Immunity* **9**, 575–585
16. Rengarajan, J., Szabo, S. J., and Glimcher, L. H. (2000) *Immunol. Today* **21**, 479–483
17. Zhang, D. H., Cohn, L., Ray, P., Bottomly, K., and Ray, A. (1997) *J. Biol. Chem.* **272**, 21597–21603
18. Zheng, W., and Flavell, R. A. (1997) *Cell* **89**, 587–596
19. Ouyang, W., Ranganath, S. H., Weindel, K., Bhattacharya, D., Murphy, T. L., Sha, W. C., and Murphy, K. M. (1998) *Immunity* **9**, 745–755
20. Lee, H. J., Takemoto, N., Kurata, H., Kamogawa, Y., Miyatake, S., O'Garra, A., and Arai, N. (2000) *J. Exp. Med.* **192**, 105–115
21. Yamashita, M., Ukai-Tadenuma, M., Miyamoto, T., Sugaya, K., Hosokawa, H., Hasegawa, A., Kimura, M., Taniguchi, M., DeGregori, J., and Nakayama, T. (2004) *J. Biol. Chem.* **279**, 26983–26990
22. Pai, S. Y., Truitt, M. L., and Ho, I. C. (2004) *Proc. Natl. Acad. Sci. U. S. A.* **101**, 1993–1998
23. Yamashita, M., Ukai-Tadenuma, M., Kimura, M., Omori, M., Inami, M., Taniguchi, M., and Nakayama, T. (2002) *J. Biol. Chem.* **277**, 42399–42408
24. Avni, O., Lee, D., Macian, F., Szabo, S. J., Glimcher, L. H., and Rao, A. (2002) *Nat. Immun.* **3**, 643–651
25. Fields, P. E., Kim, S. T., and Flavell, R. A. (2002) *J. Immunol.* **169**, 647–650
26. Inami, M., Yamashita, M., Tenda, Y., Hasegawa, A., Kimura, M., Hashimoto, K., Seki, N., Taniguchi, M., and Nakayama, T. (2004) *J. Biol. Chem.* **279**, 23123–23133
27. Omori, M., Yamashita, M., Inami, M., Ukai-Tadenuma, M., Kimura, M., Nigo, Y., Hosokawa, H., Hasegawa, A., Taniguchi, M., and Nakayama, T. (2003) *Immunity* **19**, 281–294
28. Tanaka, K., and Chiba, T. (1998) *Genes Cells* **3**, 499–510
29. Ciechanover, A. (1998) *EMBO J.* **17**, 7151–7160
30. Laney, J. D., and Hochstrasser, M. (1999) *Cell* **97**, 427–430
31. Ben-Neriah, Y. (2002) *Nat. Immun.* **3**, 20–26
32. Liu, Y. C. (2004) *Annu. Rev. Immunol.* **22**, 81–127
33. Rock, K. L., and Goldberg, A. L. (1999) *Annu. Rev. Immunol.* **17**, 739–779
34. Karin, M., and Ben-Neriah, Y. (2000) *Annu. Rev. Immunol.* **18**, 621–663
35. Takeda, K., Tanaka, T., Shi, W., Matsumoto, M., Minami, M., Kashiwamura, S., Nakanishi, K., Yoshida, N., Kishimoto, T., and Akira, S. (1996) *Nature* **380**, 627–630
36. Swan, K. A., Alberola-Ila, J., Gross, J. A., Appleby, M. W., Forbush, K. A., Thomas, J. F., and Perlmutter, R. M. (1995) *EMBO J.* **14**, 276–285
37. Kimura, M., Koseki, Y., Yamashita, M., Watanabe, N., Shimizu, C., Katsumoto, T., Kitamura, T., Taniguchi, M., Koseki, H., and Nakayama, T. (2001) *Immunity* **15**, 275–287
38. Leon, R. P., Hedlund, T., Meech, S. J., Li, S., Schaack, J., Hunger, S. P., Duke, R. C., and DeGregori, J. (1998) *Proc. Natl. Acad. Sci. U. S. A.* **95**, 13159–13164
39. Oh-hora, M., Ogata, M., Mori, Y., Adachi, M., Imai, K., Kosugi, A., and Hamaoka, T. (1999) *J. Immunol.* **163**, 1282–1288
40. Iritani, B. M., Forbush, K. A., Farrar, M. A., and Perlmutter, R. M. (1997) *EMBO J.* **16**, 7019–7031
41. Favata, M. F., Horiuchi, K. Y., Manos, E. J., Daulerio, A. J., Stradley, D. A., Feeser, W. S., Van Dyk, D. E., Pitts, W. J., Earl, R. A., Hobbs, F., Copeland, R. A., Magolda, R. L., Scherle, P. A., and Trzaskos, J. M. (1998) *J. Biol. Chem.* **273**, 18623–18632
42. Suzuki, H., Chiba, T., Kobayashi, M., Takeuchi, M., Furuichi, K., and Tanaka, K. (1999) *Biochem. Biophys. Res. Commun.* **256**, 121–126
43. Lovett-Racke, A. E., Rocchini, A. E., Choy, J., Northrop, S. C., Hussain, R. Z., Ratts, R. B., Sikder, D., and Racke, M. K. (2004) *Immunity* **21**, 719–731
44. Li, Y. Q., Hii, C. S., Der, C. J., and Ferrante, A. (1999) *Immunology* **96**, 524–528
45. Pickart, C. M. (2004) *Cell* **116**, 181–190
46. Joazeiro, C. A., and Weissman, A. M. (2000) *Cell* **102**, 549–552
47. Honda, R., and Yasuda, H. (2000) *Oncogene* **19**, 1473–1476
48. Fang, S., Jensen, J. P., Ludwig, R. L., Vousden, K. H., and Weissman, A. M. (2000) *J. Biol. Chem.* **275**, 8945–8951
49. Michael, D., and Oren, M. (2003) *Semin. Cancer Biol.* **13**, 49–58
50. Ouyang, W., Lohning, M., Gao, Z., Assenmacher, M., Ranganath, S., Radbruch, A., and Murphy, K. M. (2000) *Immunity* **12**, 27–37
51. Honda, R., Tanaka, H., and Yasuda, H. (1997) *FEBS Lett.* **420**, 25–27

52. Prives, C., and Manley, J. L. (2001) *Cell* **107,** 815–818
53. Brooks, C. L., and Gu, W. (2003) *Curr. Opin. Cell Biol.* **15,** 164–171
54. Tao, W., and Levine, A. J. (1999) *Proc. Natl. Acad. Sci. U. S. A.* **96,** 6937–6941
55. Li, M., Brooks, C. L., Wu-Baer, F., Chen, D., Baer, R., and Gu, W. (2003) *Science* **302,** 1972–1975
56. Sears, R., Nuckolls, F., Haura, E., Taya, Y., Tamai, K., and Nevins, J. R. (2000) *Genes Dev.* **14,** 2501–2514
57. Sears, R., Leone, G., DeGregori, J., and Nevins, J. R. (1999) *Mol. Cell* **3,** 169–179
58. Brondello, J. M., Pouyssegur, J., and McKenzie, F. R. (1999) *Science* **286,** 2514–2517
59. Fuchs, S. Y., Tappin, I., and Ronai, Z. (2000) *J. Biol. Chem.* **275,** 12560–12564
60. Persons, D. L., Yazlovitskaya, E. M., and Pelling, J. C. (2000) *J. Biol. Chem.* **275,** 35778–35785
61. She, Q. B., Chen, N., and Dong, Z. (2000) *J. Biol. Chem.* **275,** 20444–20449
62. Towatari, M., May, G. E., Marais, R., Perkins, G. R., Marshall, C. J., Cowley, S., and Enver, T. (1995) *J. Biol. Chem.* **270,** 4101–4107
63. Morimoto, T., Hasegawa, K., Kaburagi, S., Kakita, T., Wada, H., Yanazume, T., and Sasayama, S. (2000) *J. Biol. Chem.* **275,** 13721–13726
64. Chen, C. H., Zhang, D. H., LaPorte, J. M., and Ray, A. (2000) *J. Immunol.* **165,** 5597–5605

Regulation of T helper type 2 cell differentiation by murine Schnurri-2

Motoko Y. Kimura,[1] Hiroyuki Hosokawa,[1] Masakatsu Yamashita,[1] Akihiro Hasegawa,[1] Chiaki Iwamura,[1] Hiroshi Watarai,[1] Masaru Taniguchi,[2] Tsuyoshi Takagi,[3] Shunsuke Ishii,[3] and Toshinori Nakayama[1]

[1]Department of Immunology, Graduate School of Medicine, Chiba University, Chiba 260-8670, Japan
[2]Laboratory for Immune Regulation, RIKEN Research Center for Allergy and Immunology, Yokohama 230-0045, Japan
[3]Laboratory of Molecular Genetics, RIKEN Tsukuba Institute, Ibaraki 305-0074, Japan

Schnurri (Shn) is a large zinc finger protein implicated in cell growth, signal transduction, and lymphocyte development. Vertebrates possess at least three Shn orthologues (Shn-1, Shn-2, and Shn-3), which appear to act within the bone morphogenetic protein, transforming growth factor β, and activin signaling pathways. However, the physiological functions of the Shn proteins remain largely unknown. In Shn-2–deficient mice, mature peripheral T cells exhibited normal anti–T cell receptor–induced proliferation, although there was dramatic enhancement in the differentiation into T helper type (Th)2 cells and a marginal effect on Th1 cell differentiation. Shn-2–deficient developing Th2 cells showed constitutive activation of nuclear factor κB (NF-κB) and enhanced GATA3 induction. Shn-2 was able to compete with p50 NF-κB for binding to a consensus NF-κB motif and inhibit NF-κB–driven promoter activity. Thus, Shn-2 plays a crucial role in the control of Th2 cell differentiation by regulating NF-κB function.

The Journal of Experimental Medicine

CORRESPONDENCE
Toshinori Nakayama:
tnakayama@faculty.chiba-u.jp

Abbreviations used: BMDC, bone marrow–derived DC; CFSE, carboxyfluorescein diacetate succinimidyl ester; EMSA, electrophoretic mobility shift assay; Shn, Schnurri; Tg, transgenic; TRAF, TNF receptor–associated factor.

CD4 T cell–dependent immune responses are controlled by the balance of antigen-specific Th1 and Th2 cells (1–3). IL-12–induced activation of STAT4 is crucial for Th1 cell differentiation, whereas IL-4–induced STAT6 activation is crucial for Th2 cell differentiation (4–8). In addition to cytokine-induced signals, the activation of the TCR-mediated signaling is indispensable for both Th1 and Th2 cell differentiation. In particular, Th2 cell differentiation is largely dependent on the activation of p56^{lck}, calcineurin, and the Ras-ERK MAPK signaling cascade (9–11). A negative regulator of the above signaling pathways, SHP-1, also controls the efficiency of Th2 cell differentiation and Th2 cell–dependent immune responses (12). Master transcription factors for Th1 and Th2 cell differentiation have been revealed, i.e., GATA3 for Th2 cells and T-bet for Th1 cells (13–17).

In Drosophila, Mad-Medea and Schnurri (Shn), a large zinc finger protein, are reported to interact with each other and act as nuclear targets in the Drosophila decapentaplegic signaling pathway (18–20). In vertebrates, the Drosophila decapentaplegic signaling pathway

may equate to the bone morphogenetic protein/TGF-β/activin signaling pathways that play diverse roles in developmental processes (21). Vertebrates have at least three orthologues of Shn: Shn-1 (also known as HIV-EP1, MBP-1, PRDII-BF1, and αA-CRYBP1), Shn-2 (also known as HIV-EP2, MBP-2, AGIE-BP1, and MIBP1), and Shn-3 (also known as HIV-EP3, KRC, and ZAS3). The mRNA expression of Shn-2 was detected mostly in the brain, heart, and spleen (22–24). Recently, the requirement of Shn-2 in positive selection of thymocytes was reported (25) and Shn-3–deficient CD4^{+} CD8^{+} thymocytes were shown to exhibit a defect in cell survival (26). However, the precise physiological roles of these Shn family members remain largely unknown.

NF-κB is a critical transcription factor that regulates Th2 cell differentiation and Th2 cell–dependent airway inflammation (27–29). NF-κB–deficient (p50 subunit–deficient) mice were unable to mount OVA-induced airway inflammation (28). The lack of inflammation was not due to defects in T cell priming, T cell proliferation, or expression of important cell adhesion molecules, but rather to the impaired induction of GATA3 (30). Recently, one of the Shn family members, Shn-3 (KRC), was

The online version of this article contains supplemental material.

397

reported to associate with TNF receptor–associated factor (TRAF)2 to repress nuclear translocation of NF-κB (31). In addition, Shn-3 (ZAS3) was shown to bind to the NF-κB

motif directly, and the competition with NF-κB binding resulted in the repression of transactivation of the NF-κB target gene (32, 33). A direct repressive activity of Shn-3 was
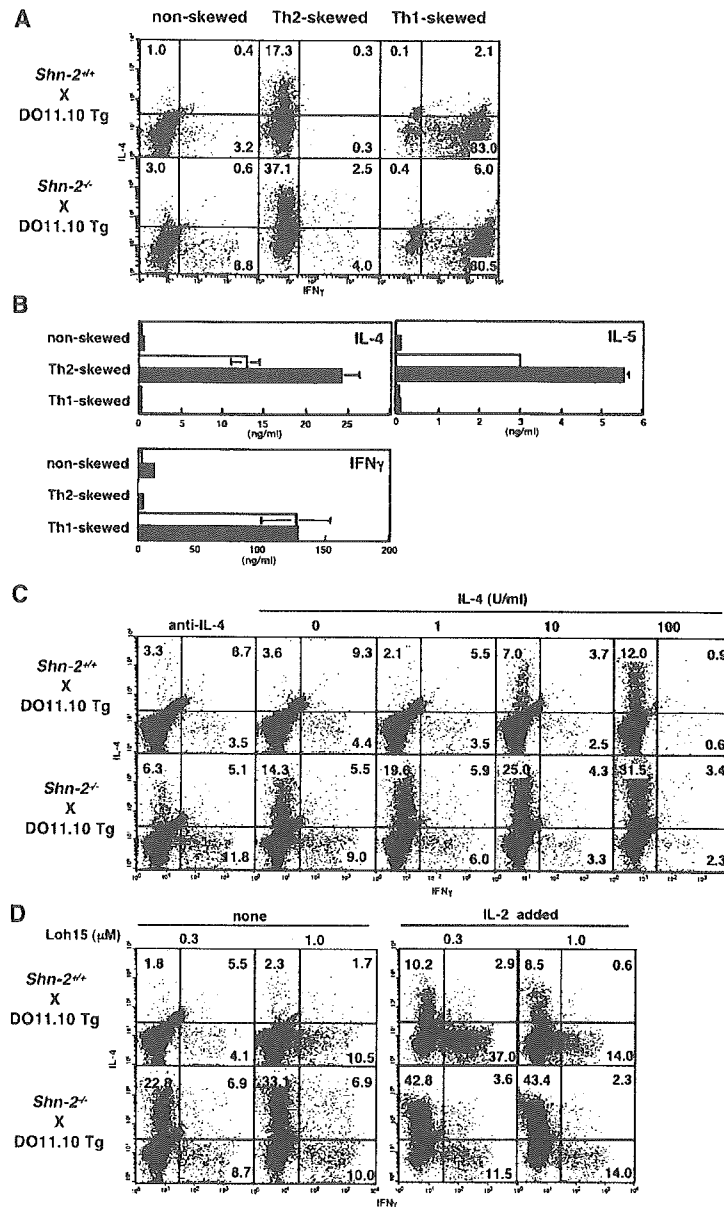

Figure 1. Enhanced Th2 cell differentiation in *Shn-2* / × DO11.10 TCR Tg T cells. (A) Naive (CD44^low) CD4 T cells from *Shn-2* -/- × DO11.10 Tg mice were purified by cell sorting and stimulated with antigenic OVA peptide (Loh15: 0.1 μM) and irradiated BALB/c APCs for 5 d. Th2 cell–skewed (IL-4 with anti–IL-12 mAb and anti–IFN-γ mAb), Th1 cell–skewed (IL-12 with anti–IL-4 mAb), and nonskewed (IL-2 with anti–IL-4 mAb, anti–IL-12 mAb, and anti–IFN-γ mAb) conditions were used. Intracellular staining was performed with FITC-conjugated anti–IFN-γ mAb and PE-conjugated anti–IL-4 mAb. Under the typical Th2 cell–skewed conditions, the levels of Th2 cell differentiation in five experiments were 17.5 ± 2.9% in *Shn-2*^+/+ cultures and 38.0 ± 11.8% in *Shn-2* -/- cultures. P < 0.006. (B) A portion of

the same differentiated cell cultures used in A were restimulated with antigenic peptide and APCs for 24 h, and the concentrations of cytokines (IL-4, IL-5, and IFN-γ) in the culture supernatant were determined by ELISA. (C) Naive (CD44^low) CD4 T cells from *Shn-2* -/- × DO11.10 Tg mice were stimulated with a specific OVA peptide (Loh15: 0.1 μM) and irradiated normal BALB/c APCs in the presence of indicated doses of IL-4. Intracellular staining profiles of IFN-γ and IL-4 are shown with percentages of cells in each area. (D) Purified naive (CD44^low) CD4 T cells were stimulated with indicated doses of specific OVA peptides (Loh15: 0.3 and 1.0 μM) and irradiated BALB/c APCs in the presence or absence of 30 U/ml of exogenous IL-2. Two independent experiments were performed with similar results.

398

also demonstrated (33). These emerging findings suggest that the Shn protein is involved in NF-κB activation and/or NF-κB–mediated gene transactivation.

Here, we investigate the role of Shn-2 in Th1/Th2 cell differentiation by using Shn-2–deficient (Shn-$2^{-/-}$) mice. Our results suggest that Shn-2 plays crucial roles in the control of Th2 cell differentiation by regulating NF-κB activation and GATA3 expression.

RESULTS

Phenotypic and functional characterization of peripheral CD4 T cells in Shn-2–deficient (Shn-$2^{-/-}$) mice

Shn-$2^{-/-}$ mice were previously shown to have a defect in T cell generation due to the impairment of positive thymic selection (25). However, we found that moderate numbers of CD4 and CD8 T cells were present in Shn-$2^{-/-}$ mice of a BALB/c background (Fig. S1 A, available at http://www.jem.org/cgi/content/full/jem.20040733/DC1). The cell surface expression of TCR-β, CD3ε, common γ (γC), IL-4Rα, CD25, CD69, CD44, and CD62L on splenic CD4 T cells was found to be comparable to those of controls (Fig. S1 B). The TCR Vβ chain repertoire in the peripheral Shn-$2^{-/-}$ T cells was similar to that of Shn-$2^{+/+}$ T cells (Fig. S1 C). Anti–TCR-β– or anti–CD3ε–induced proliferative responses were the same in Shn-$2^{+/+}$ and Shn-$2^{-/-}$ CD4 T cells (Fig. S2 A). Furthermore, the phosphorylation status of MAPKs (Erk1 and Erk2) after TCR cross-linking in Shn-$2^{-/-}$ CD4 T cells was comparable to that of controls (Fig. S2 B). Thus, no obvious defect in the phenotype or the activation of Shn-$2^{-/-}$ splenic CD4 T cells was noted. The expression of Shn-2 mRNA was detected in freshly prepared CD4 T cells, and it was decreased after anti-TCR stimulation in Th1 and Th2 cell differentiation cultures (Fig. S3).

Enhanced Th2 cell differentiation in Shn-$2^{-/-}$ × DO11.10 transgenic (Tg) naive CD4 T cells

Next, we assessed the capability of Shn-$2^{-/-}$ CD4 T cells to differentiate into Th1/Th2 cells. Naive splenic CD4 T cells (CD4^{+} CD44^{low}) were purified by cell sorting (purity >98%) and then subjected to in vitro Th1/Th2 cell differentiation culture and analyzed by intracellular cytokine staining and ELISA. Naive CD4 T cells from Shn-$2^{-/-}$ × OVA–specific TCR-αβ Tg (DO11.10 Tg) mice were stimulated with 0.1 μM of antigenic OVA peptide and irradiated BALB/c splenocytes in the presence of appropriate cytokines and anti-cytokine mAbs under three different conditions: Th2-skewed (IL-4 with anti–IL-12 mAb and anti–IFN-γ mAb), Th1-skewed (IL-12 with anti–IL-4 mAb), and nonskewed (IL-2 with anti–IL-4 mAb, anti–IL-12 mAb, and anti–IFN-γ mAb) conditions. As shown in Fig. 1 A, Th2 cell differentiation was enhanced substantially in Shn-$2^{-/-}$ T cells (17.3 vs. 37.1%), whereas Th1 cell differentiation was unaffected (83.0 vs. 80.5%). Under nonskewed conditions, the baseline levels of IL-4–producing and IFN-γ–producing cells were increased in Shn-$2^{-/-}$ T cell cultures (Fig. 1 A, left). Portions of the same cell cul-

tures that were used for intracellular cytokine staining were restimulated, and cytokine production was measured by ELISA. Basically, a similar pattern among cultures was observed (Fig. 1 B). The production of IL-4 and IL-5 was increased about twofold in Shn-$2^{-/-}$ Th2 cells, whereas similar levels of IFN-γ production in Th1 cells were detected. The levels of IL-4 and IFN-γ production in nonskewed cultures were very low, but they were slightly increased in the Shn-$2^{-/-}$ cultures.

To examine further the effect on Th2 cell differentiation, naive CD4 T cells from Shn-$2^{-/-}$ × DO11.10 Tg mice were stimulated with a minimum dose of antigenic peptide (0.1 μM) and APCs in the presence of graded doses of exogenous IL-4. As shown in Fig. 1 C, IL-4–producing Th2 cells were generated in an exogenous IL-4 dose-dependent manner in wild-type Shn-$2^{+/+}$ T cell cultures. As expected, the generation of Th2 cells in Shn-$2^{-/-}$ mice was dramatically enhanced at all doses of exogenous IL-4. The number of IL-5–producing cells was also enhanced in Shn-$2^{-/-}$ T cell cultures (not depicted). Also, we detected increased numbers of IFN-γ–producing cells at all groups. Next, we examined the effect of the concentration of antigenic peptide and IL-2 in the culture. Naive CD4 T cells purified by cell sorting were stimulated with two different doses of antigenic peptide (0.3 or 1.0 μM) and irradiated APCs from normal BALB/c mice in the absence of exogenous IL-4. A dramatic increase in the numbers of IL-4–producing Th2 cells was observed in Shn-$2^{-/-}$ cultures at either dose of antigenic peptide (Fig. 1 D, left). In the presence of exogenous IL-2, Th2 cell generation was enhanced in both Shn-$2^{+/+}$ and Shn-$2^{-/-}$ T cell cultures, although the levels were substantially higher in Shn-$2^{-/-}$ groups as compared with Shn-$2^{+/+}$.

Enhanced Th2 cell differentiation in Shn-$2^{-/-}$ splenic CD4 T cells after anti-TCR mAb stimulation

To further assess the efficiency of Th2 cell differentiation in the splenic Shn-$2^{-/-}$ T cells, purified splenic naive CD4 T cells (purity >98%) were stimulated with immobilized anti–TCR-β mAb in the presence of graded doses of exogenous IL-4. No APCs were added. 30 U/ml of exogenous IL-2 was added to the differentiation cultures. As shown in Fig. 2 A, IL-4–producing Th2 cells were generated in an exogenous IL-4 dose-dependent manner in the Shn-$2^{+/+}$ wild-type T cell cultures, and as expected, the generation of Th2 cells in Shn-$2^{-/-}$ mice was substantially enhanced in the cultures at all doses of exogenous IL-4 (Fig. 2 A). These results suggest that the ability to differentiate into Th2 cells was enhanced in Shn-$2^{-/-}$ splenic CD4 T cells. The number of Th2 cells generated in Shn-$2^{-/-}$ × $STAT6^{-/-}$ T cell cultures was insignificant, suggesting that the enhanced Th2 cell differentiation in Shn-$2^{-/-}$ T cell cultures was STAT6 dependent (not depicted).

To assess the effect on Th1 cell differentiation in a non-TCR Tg system, Shn-$2^{-/-}$ splenic CD4 T cells were stimulated with anti–TCR-β mAb in the presence of various doses of exogenous IL-12 and anti–IL-4 mAb (Fig. 2 B).
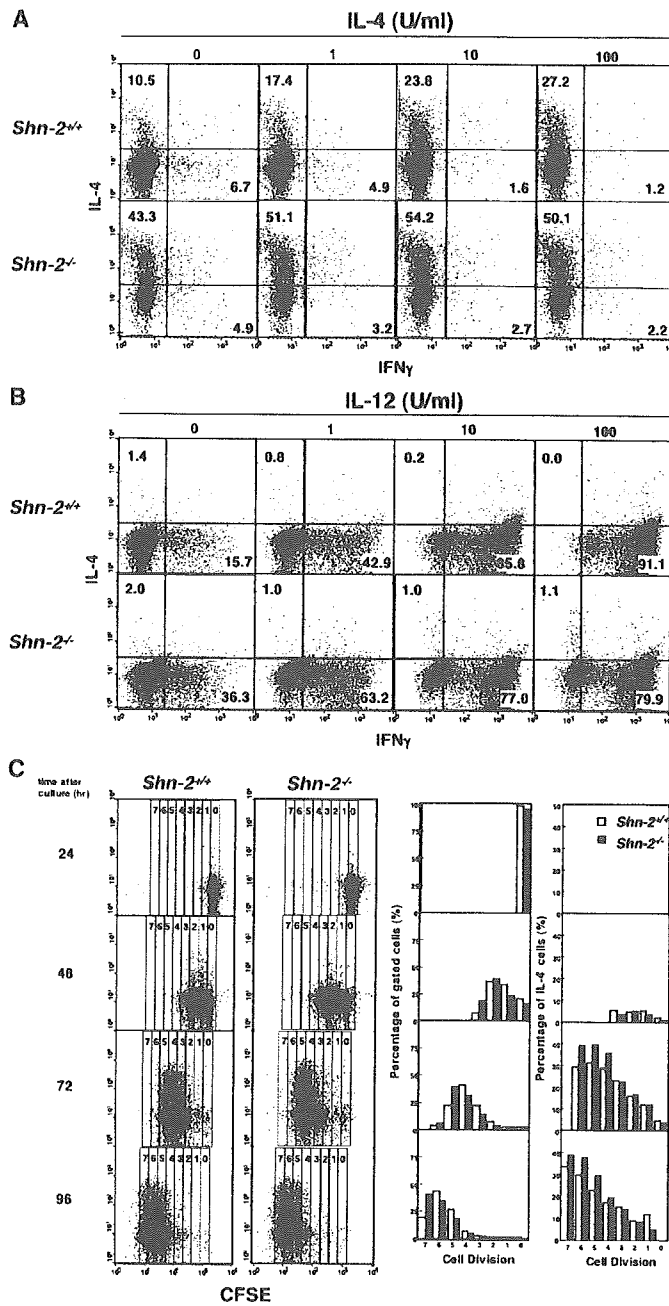
Figure 2. Enhanced Th2 cell differentiation in *Shn-2 -/-* T cells.
(A) Splenic naive CD4 T cells from *Shn-2 -/-* mice were stimulated with immobilized anti-TCR-β mAb, 30 U/ml of exogenous IL-2, and indicated concentrations of IL-4 for 5 d. Intracellular staining profiles of IFN-γ and IL-4 are shown with percentages of cells in each area. The absolute numbers of cells harvested in these cultures were similar. Three independent experiments were performed with similar results. (B) Splenic naive CD4 T cells from *Shn-2 -/-* mice were stimulated with immobilized anti-TCR-β mAb in the presence of indicated doses of IL-12 and anti-IL-4 mAb. Intracellular staining profiles of IFN-γ and IL-4 are shown with percentages of cells in each area. The absolute numbers of cells harvested in these cultures were

similar. Three independent experiments were performed with similar results. (C) Splenic naive CD4 T cells were labeled with CFSE and stimulated with immobilized anti-TCR-β mAb in the presence of IL-4 and IL-2. After culturing for the indicated times, cells were restimulated and subjected to intracellular staining with APC-conjugated anti-IL-4 mAb. Percentages of the cells in the gates representing numbers of cell division (0-7) and percentages of IL-4-producing Th2 cells in each gate are shown in the right panels. Percentages of IL-4-producing cells in total (without gating) are 0.7% (24 h), 5.4% (48 h), 28.6% (72 h), and 29.3% (96 h) in *Shn-2 +/+* cultures and 0.6% (24 h), 5.4% (48 h), 36.9% (72 h), and 37.9% (96 h) in *Shn-2 -/-* cells. Two independent experiments were performed with similar results.
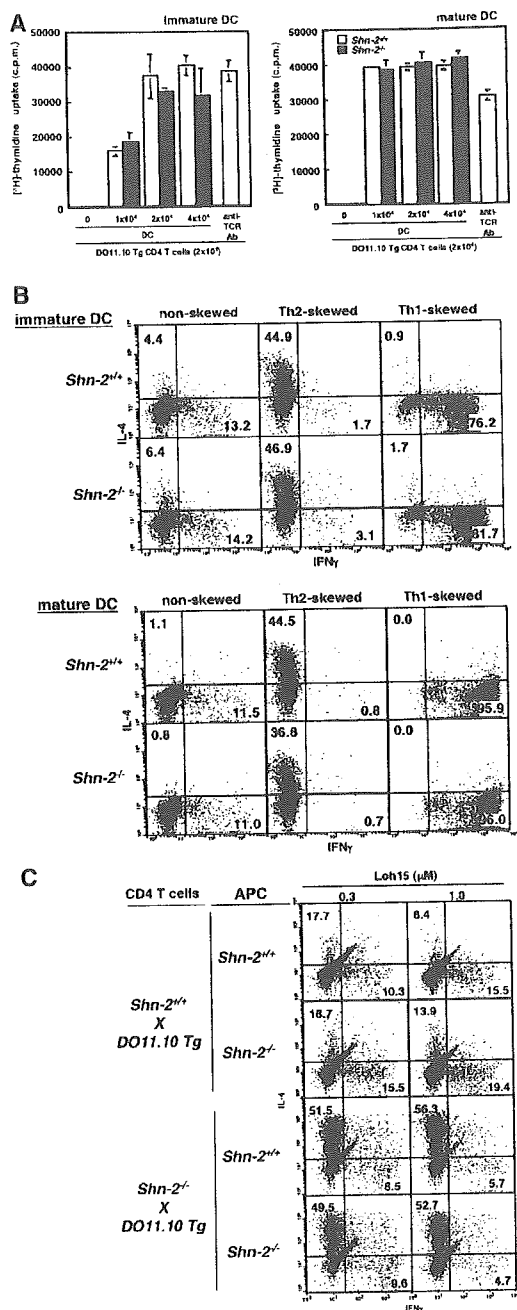
400

Moderate increases in the generation of Th1 cells were observed in groups with no exogenous IL-12 or a low dose of IL-12 (1 U/ml). However, no further increases but rather a slight decrease in the number of Th1 cells generated was observed at higher doses of IL-12 (10 or 100 U/ml). A similar pattern was obtained in STAT6-deficient Th1 cell cultures (not depicted). We observed similar enhancement in the generation of Th2 cells in $Shn-2^{-/-}$ mice with either a B6 background or a B6 × BALB/c background (not depicted).

Anti-TCR–induced cell division of $Shn-2^{-/-}$ CD4 T cells

Because some cycles of cell divisions are reported to be required for the generation of IL-4–producing Th2 cells (34), we examined the anti-TCR–induced cell division of $Shn-2^{-/-}$ CD4 T cells. Carboxyfluorescein diacetate succinimidyl ester (CFSE)-labeled naive CD4 T cells were stimulated with anti-TCR-β mAb in the presence of IL-2 and IL-4 (Th2 cell–skewed condition), and 24, 48, 72, and 96 h later, IL-4 production in the developing Th2 cells was assessed (Fig. 2 C). 24 h after the stimulation, most cells had not undergone cell division (cell division no. 0), and IL-4–producing Th2 cells were not detected. At 48 h, cells had undergone up to three cell divisions, and there was a slight increase in the numbers of cells with three cell divisions detected in $Shn-2^{-/-}$ CD4 T cells. The percentages of IL-4–producing T cells generated were not apparently different between $Shn-2^{-/-}$ and $Shn-2^{+/+}$ CD4 T cell cultures at this time point. After 72 and 96 h in culture, the rate of cell division appeared to be slightly increased in $Shn-2^{-/-}$ CD4 T cells, and the generation of IL-4–producing T cells was higher at all numbers of cell division. These results suggest that although $Shn-2^{-/-}$ CD4 T cells show a slightly increased rate in cell division, the enhanced Th2 cell generation in $Shn-2^{-/-}$ CD4 T cells could not be simply explained by the difference in the number of cell divisions that the developing Th2 cells had undergone.

We reported previously that CD28 costimulation induced increased Th2 cell differentiation (35) and induced NF-κB activation and enhanced GATA3 expression in developing Th2 cells to facilitate chromatin remodeling of the IL-5 gene loci (36). $Shn-2^{-/-}$ T cells were stimulated with anti-TCR plus anti-CD28 mAb under Th2 cell–skewed conditions (Fig. S4, available at http://www.jem.org/cgi/content/full/jem.20040733/DC1). $Shn-2^{-/-}$ T cells showed increased levels of Th2 cell differentiation without anti-CD28 mAb as compared with wild-type (46.2 vs. 32.4%). No obvious additional enhancement of Th2 cell differentiation was detected in the presence of CD28 costimulation under the conditions where the CD28-mediated enhancing effect was observed in $Shn-2^{+/+}$ T cell cultures.

Figure 3. The function of $Shn-2^{-/-}$ APCs. (A) OVA-pulsed immature or mature BMDCs were cocultured with DO11.10 Tg CD4 T cells for 72 h. [3H]thymidine (37 kBq/well) was added to the stimulation culture for the last 16 h. The results (mean and standard deviation) of [3H]thymidine incorporation are shown. Three independent experiments were performed with similar results. (B) OVA-pulsed immature or mature BMDCs (2 × 10⁴ cells) were cocultured with DO11.10 Tg naive (CD44^low) CD4 T cells (2 × 10⁵ cells) under nonskewed, Th2 cell–skewed, and Th1 cell–skewed conditions for 5 d. Intracellular staining profiles (IFN-γ/IL-4) of the cultured cells are shown with percentages of the cells in each quadrant. Three independent experiments were performed with similar results. (C) Naive (CD44^low) CD4 T

cells (1.5 × 10⁴ cells) were purified from $Shn-2^{-/-}$ × DO11.10 Tg mice by cell sorting and stimulated with indicated doses of specific OVA peptides (Loh15: 0.1 μM) and irradiated CD4⁻ spleen cells (10⁵ cells) from non-DO11.10 Tg $Shn-2^{+/+}$ or $Shn-2^{-/-}$ mice. Two independent experiments were performed with similar results.

No functional defect was observed in DCs from *Shn-2⁻/⁻* mice

The results thus far suggested that the observed enhancement of Th2 cell differentiation is due to an alteration in T cells because we used purified T cells (Figs. 1 and 2) and APCs from normal mice (Fig. 1). However, *Shn-2* mRNA is expressed in both CD4 T cells and APCs (not depicted), and thus, we wished to evaluate the effect of *Shn-2* deficiency on APC function using bone marrow–derived DCs (BMDCs). The expression levels of CD11c, I-A^d, H-2K^d, CD40, B7-1, B7-2, and Fas were comparable between *Shn-2⁺/⁺* and *Shn-2⁻/⁻* BMDCs (not depicted). OVA-pulsed BMDCs from *Shn-2⁺/⁺* or *Shn-2⁻/⁻* mice were cocultured with DO11.10 Tg CD4 T cells, and proliferative responses of T cells were assessed by [^{3}H]thymidine uptake. Under these conditions, the APC function of both immature and mature BMDCs was found to be comparable between *Shn-2⁻/⁻* or *Shn-2⁺/⁺* mice (Fig. 3 A). We then examined the ability of OVA-pulsed BMDCs as APCs to induce Th1/Th2 cell differentiation. Stimulation with either immature or mature BMDCs resulted in similar levels of Th1/Th2 cell differentiation in the cultures with *Shn-2⁺/⁺* and *Shn-2⁻/⁻* BMDCs (Fig. 3 B).

To further evaluate the APC function of *Shn-2⁻/⁻* mice, spleen cells were irradiated and tested for their ability to induce Th1/Th2 cells. The numbers of Th2 cells generated were found to be comparable between cultures with *Shn-2⁻/⁻* and *Shn-2⁺/⁺* APCs (Fig. 3 C). Taken together, the enhanced Th2 cell generation in *Shn-2⁻/⁻* T cell cultures appears to be due to an alteration in CD4 T cells themselves and not to any change in APC function.

Hyperactivation of NF-κB in *Shn-2⁻/⁻* CD4 T cells

We examined the NF-κB activation in *Shn-2⁻/⁻* CD4 T cells by electrophoretic mobility shift assays (EMSAs). CD4 T cells from *Shn-2⁺/⁺* and *Shn-2⁻/⁻* mice were stimulated with anti-TCR and anti-CD28 for 3 h, and subsequently, nuclear extracts were prepared. To facilitate the stimulation of the TCR complex on naive T cells, we used both anti-TCR and anti-CD28 mAbs. The NF-κB DNA binding activity was found to be increased after TCR stimulation in *Shn-2⁺/⁺* CD4 T cells (Fig. 4 A, lanes 2 and 3, and B, lanes 2 and 14). In contrast, in *Shn-2⁻/⁻* CD4 T cells, substantial levels of binding activity could already be detected even in nonstimulated T cells (Fig. 4 A, lane 4, and B, lanes 7 and 17), and an only
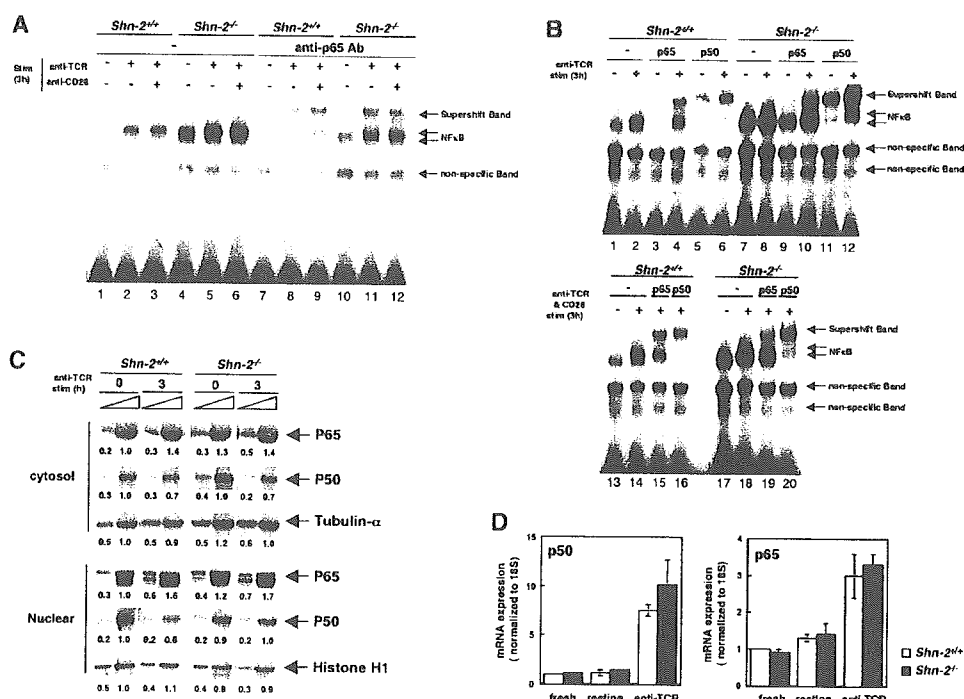

Figure 4. Hyperactivation of NF-κB in *Shn-2⁻/⁻* CD4 T cells.
(A and B) Splenic CD4 T cells were incubated with medium alone overnight and then stimulated with immobilized anti-TCR-αβ mAb in the presence or absence of agonistic anti-CD28 antibody for 3 h. Nuclear extracts of the cultured cells were prepared and subjected to EMSAs with NF-κB probes. The supershift assays were performed with antibodies specific for NF-κB p50 and p65 subunit detection. Three independent experiments were performed with similar results. (C) Splenic CD4 T cells were incubated with medium alone overnight and then stimulated with immobilized anti-TCR-β

mAb for 3 h. Subsequently, both cytosol and nuclear extracts were prepared and these were subjected to immunoblotting using anti-p50, anti-p65, anti-tubulin-α, and anti-histone H1 antibodies. Arbitrary densitometric units are shown under each band. (D) RNAs were prepared from fresh splenic CD4 T cells, resting CD4 T cells that were incubated with medium alone overnight, and anti-TCR-stimulated CD4 T cells, and then quantitative PCR assay was performed. The expression levels of p50 and p65 were normalized with 18S expression. Two independent experiments were performed with similar results.

— 90 —

moderate elevation in activity was observed after TCR stimulation (Fig. 4 A, lanes 5 and 6, and B, lanes 8 and 18). We performed a supershift assay to determine the specificity for NF-κB subunits and observed a substantial supershift with the anti-p65 antibody (Fig. 4 A, lanes 8 and 9, and B, lanes 4 and 15). A small, but reproducible shift was detected in $Shn-2^{-/-}$ nonstimulated samples (Fig. 4 A, lane 10, and B, lane 9). Increased amounts of p65 supershift band were detected after anti-TCR stimulation in $Shn-2^{-/-}$ T cells. Furthermore, an EMSA with anti-p50 antibody revealed that most of the NF-κB EMSA band detected in nonstimulated $Shn-2^{-/-}$ T cells contained the p50 subunit (Fig. 4 B, lane 11). There was a substantial increase in the level of the p50 band after anti-TCR stimulation (Fig. 4 B, lane 12). These results suggest that NF-κB is constitutively activated in $Shn-2^{-/-}$ CD4 T cells and it is hyperactivated after anti-TCR stimulation. We did not observe any obvious disappearance of specific bands in $Shn-2^{-/-}$ groups. This could be due to an insufficient amount of Shn-2 for visualization in the EMSA assay.

An assessment of the protein expression levels of NF-κB p50 and p65 subunits in the cytosol and in nuclear fractions revealed that no obvious difference was detected between $Shn-2^{+/+}$ and $Shn-2^{-/-}$ T cells before or after anti-TCR stimulation, suggesting that the nuclear translocation of the NF-κB p50 and p65 subunits is not altered in the absence of Shn-2 (Fig. 4 C). Furthermore, transcriptional levels of p50 and p65 were compared by quantitative RT-PCR assay using freshly prepared CD4 T cells, resting CD4 T cells, and those after anti-TCR stimulation for 3 h (Fig. 4 D). In all

cases, basically no difference was detected between $Shn-2^{+/+}$ and $Shn-2^{-/-}$ groups.

We also examined the activation of AP-1, CREB, and IL-4 NFAT in $Shn-2^{-/-}$ CD4 T cells by EMSA (Fig. S5, available at http://www.jem.org/cgi/content/full/jem.20040733/DC1). The DNA binding ability of AP-1 was slightly, but reproducibly, enhanced in $Shn-2^{-/-}$ T cells, whereas the DNA binding activity of CREB and IL-4 NFAT appeared to be similar in $Shn-2^{+/+}$ and $Shn-2^{-/-}$ T cells.

Enhanced expression of GATA3 in anti–TCR–activated $Shn-2^{-/-}$ CD4 T cells

Because the levels of GATA3 expression are critical for Th2 cell differentiation (14) and because GATA3 expression is regulated by NF-κB (30), we next assessed the protein expression of GATA3 in cultured $Shn-2^{-/-}$ T cells under Th2 cell–skewed condition. Splenic CD4 T cells from $Shn-2^{-/-}$ mice were stimulated with anti–TCR–β mAb and IL-4, and 16 h later, the expression of GATA3 was assessed by immunoblotting with specific antibodies. The levels of GATA3 protein were found to be reproducibly increased in $Shn-2^{-/-}$ T cells (Fig. 5 A). No detectable GATA3 protein was observed in freshly prepared $Shn-2^{-/-}$ CD4 T cells (not depicted). Concurrently, the mRNA levels were assessed by semiquantitative RT-PCR analysis, and increased GATA3 mRNA levels were detected (Fig. 5 B). These results suggest that enhanced induction of GATA3 takes place in early developing $Shn-2^{-/-}$ Th2 cells as compared with that of control $Shn-2^{+/+}$ Th2 cells.
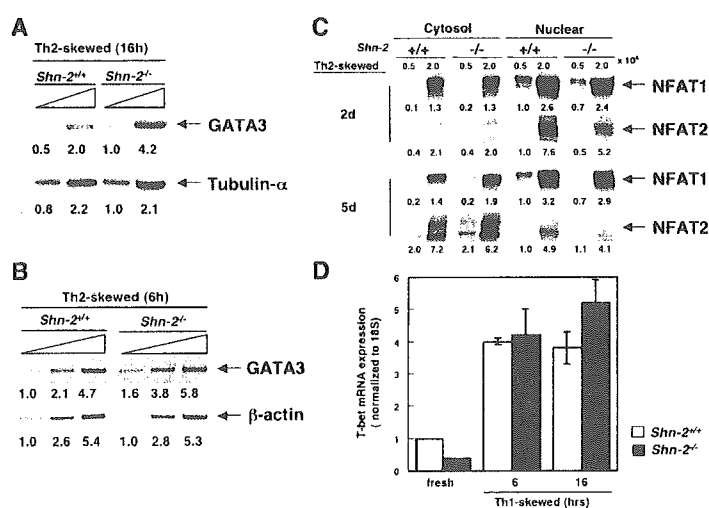
Figure 5. Increased GATA3 expression in $Shn-2^{-/-}$ developing Th2 cells. (A) Splenic CD4 T cells were cultured under Th2 cell–skewed conditions for 16 h. The cells were lysed, and cell lysates with threefold serial dilutions of cell lysates were subjected to immunoblotting using anti-GATA3 or anti–tubulin-α antibodies. Arbitrary densitometric units are shown under each band. (B) Splenic CD4 T cells were cultured under Th2 cell–skewed conditions for 6 h, and the expression levels of GATA3 mRNA were determined by RT-PCR. Arbitrary densitometric units are shown under each band. (C) Expression of NFAT1 and NFAT2 in $Shn-2^{-/-}$ Th2 cells. Splenic CD4 T cells were stimulated under Th2 cell–skewed conditions for 2 or 5 d, and then both cytosol and nuclear cell lysates were prepared. Immunoblotting was performed with anti-NFAT1 or anti-NFAT2 antibodies. Arbitrary densitometric units are shown under each band. (D) Splenic CD4 T cells were cultured under Th1 cell–skewed conditions for 6 or 16 h, and the expression levels of T-bet mRNA were determined by quantitative PCR assay. The expression was normalized with 18S expression. Two independent experiments were performed with similar results.

403

— 91 —

We examined the cytosolic or nuclear protein expression levels of NFAT1 and NFAT2 in developing Th2 cells (Fig. 5 C). In either cytosolic or nuclear lysate, there was no clear difference in the expression of NFAT1 detected between $Shn-2^{+/+}$ and $Shn-2^{-/-}$ T cells, suggesting normal nuclear translocation of NFAT1 occurs. The nuclear translocation of NFAT2 was, however, slightly impaired in $Shn-2^{-/-}$ T cells. An assessment of the expression of other molecules that may regulate Th2 cell differentiation directly or indirectly, such as JunB, cMaf, Bcl-6, and TRAF2, revealed no clear difference in mRNA expression levels in $Shn-2^{-/-}$ developing Th2 cells (not depicted). In addition, mRNA levels of several NF-κB target genes (IL-6, IL-1β, IL-15, and IL-17) are increased in Shn-2–deficient T cells (not depicted). The levels of T-bet in the $Shn-2^{+/+}$ and $Shn-2^{-/-}$ cells cultured under Th1 cell-skewed conditions are shown in Fig. 5 D. No significant difference was observed in the levels of T-bet mRNA.

Shn-2 inhibits an NF-κB–dependent transcriptional activity

The ability of Shn-2 protein to bind to the consensus NF-κB binding motif was assessed. 293 T cells were transfected with a pAct-Flag-hShn-2 vector, and 2 d later, nuclear extracts were prepared. Biotinylated NF-κB and control AP-1 oligonucleotides were absorbed on to streptavidin-agarose beads

and incubated with the nuclear extracts. The amount of Shn-2 protein in the precipitates of agarose beads was assessed by immunoblotting with anti-Flag mAb. Total nuclear extracts were also run in parallel as loading controls. As can be seen in Fig. 6 A, a substantial binding of Flag–Shn-2 protein to NF-κB oligo was observed. This result suggests that Shn-2 protein is able to bind to a consensus NF-κB binding motif.

Next, we wished to examine whether Shn2 competes effectively with p50 NF-κB for binding to a consensus NF-κB binding motif. Nuclear extracts were prepared from 293 T cells that were transfected with pAct-Flag-hShn2 or pCMX-p50 vectors. The extracts were mixed in specific ratios and then incubated with NF-κB oligonucleotides absorbed with streptavidin-agarose beads. The bound protein was detected by immunoblotting with an anti-Flag mAb for Shn-2 and an anti-p50 mAb for p50 protein. As shown in Fig. 6 B, left, the binding of p50 to NF-κB oligonucleotides was inhibited by Shn-2–containing extracts in a dose-dependent manner. In addition, the binding of Shn-2 to NF-κB oligonucleotides was inhibited by the presence of p50 (Fig. 6 B, right). These results clearly suggest that Shn-2 competes with p50 for binding to a consensus NF-κB motif.

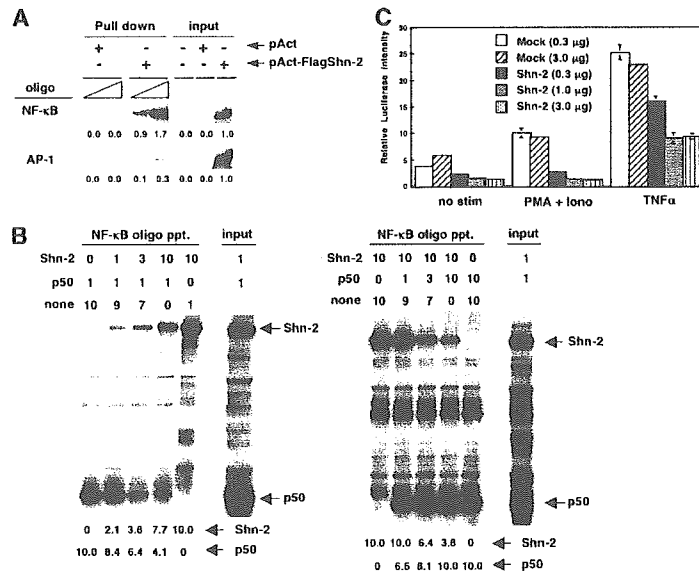Consequently, to determine whether Shn-2 protein plays a functional role in NF-κB–dependent transcription, NF-

Figure 6.   Inhibition of NF-κB–dependent transcriptional activity by Shn-2. (A) 293 T cells were transfected with a control pAct or a pAct-Flag-hShn-2 vector, and 2 d later, their cell lysates were prepared. Biotinylated NF-κB and control AP-1 oligonucleotides were absorbed by streptavidin-agarose beads, and then the beads were incubated with cell lysates. The amount of Shn-2 protein in the precipitates was assessed by immunoblotting with anti-Flag mAb. Total cell lysates (10⁶ equivalent/ lane) were also run as controls (input). Three independent experiments were performed with similar results. (B) Nuclear extracts were prepared from 293 T cells transfected with pAct-Flag-hShn2 or pCMX-p50 vectors. The extracts were mixed in a certain ratio and then incubated with NF-κB oligonucleotides absorbed with streptavidin-agarose beads. The numbers

represent the volume of cell lysates (μl; 1 μl = 5 × 10⁵ cell equivalent). none, nontransfected 293 T lysates. The bound protein was detected by immunoblotting with an anti-Flag mAb for Shn-2 and an anti-p50 mAb for p50 protein. Total cell lysates were also run as controls (input). The position of Shn-2 and p50 are indicated. Three experiments were performed with similar results. (C) 293 T cells were transfected with 25 ng of the 5× NF-κB reporter constructs with the indicated doses of a pAct control vector (Mock) or a pAct-Flag-hShn-2 vector (Shn-2). Additionally, 1 ng pRL-TK vector was added into each transfection as an internal control. 24 h after the transfection, cells were stimulated with 50 ng/ml PMA and 500 nM ionomycin or 10 ng/ml TNF-α for12 h and then assayed for luciferase activity.

TH2 CELL DIFFERENTIATION CONTROLLED BY SCHNURRI-2 | Kimura et al.

κB–induced luciferase assay was performed with 293 T cells transfected with the 5× NF-κB reporter constructs along with graded doses of pAct-Flag-hShn-2 vector after stimulation with PMA plus ionomycin or TNF-α (Fig. 6 C). Some level of luciferase activity was detected without stimulation, and a significant inhibition was observed in the presence of Shn-2. After PMA plus ionomycin stimulation, the luciferase activity was increased and this was efficiently inhibited by Shn-2 (Fig. 6 C, middle). The luciferase activity was increased dramatically by stimulation with TNF-α, and this was moderately inhibited in the presence of Shn-2 protein (Fig. 6 C, right). These results suggest that Shn-2 protein is able to inhibit the NF-κB–dependent transcriptional activity.

DISCUSSION

In this report, we demonstrated a crucial role for *Shn-2* in Th2 cell differentiation. Shn-2 appears to control NF-κB DNA binding activity and subsequent GATA3 induction in early developing Th2 cells.

The DNA binding of NF-κB was enhanced in *Shn-2*–deficient CD4 T cells (Fig. 4, A and B). The enhancement was already apparent in nonstimulated *Shn-2*–deficient CD4 T cells. However, we found the NF-κB protein equally expressed in the nucleus and cytoplasm of nonstimulated and stimulated *Shn-2*–deficient CD4 T cells (Fig. 4 C). Thus, the enhanced DNA binding of NF-κB might be regulated by nuclear events such as those involved in the DNA binding process. A previous report suggested that Shn-3 binds to a NF-κB motif and represses transactivation of NF-κB–dependent genes (33). We show here that Shn-2 protein is able to bind to a consensus NF-κB motif (Fig. 6 A) and compete with p50 for DNA binding in a dose-dependent manner (Fig. 6 B). In addition, we detected significant inhibition of the NF-κB–dependent transcriptional activity in 293 T cells. Thus, it is conceivable that Shn-2 is able to bind to NF-κB DNA binding motifs and thus compete with the binding of NF-κB complexes or to repress directly the transactivation of the NF-κB–dependent genes in early developing Th2 cells. This might be a mechanism to account for the elevated NF-κB DNA binding activity in nonstimulated *Shn-2*–deficient CD4 T cells (Fig. 4, A and B).

In addition, we detected a further enhancement of DNA binding of NF-κB after TCR stimulation (Fig. 4, A and B). This could explain the enhanced induction of GATA3 in early developing *Shn-2*−/− Th2 cells (Fig. 5, A and B). A similar regulation was demonstrated in an experimental system using p50−/− mice (30). In our preliminary results, the generation of IL-4–producing Th2 cells in wild-type BALB/c CD4 T cell cultures was increased by the ectopic expression of both p50 and p65 (unpublished data). Thus, it appears probable that the enhanced induction of GATA3 by NF-κB hyperactivation is a mechanism that is responsible for the enhanced Th2 cell differentiation observed in Shn-2–deficient T cells.

Another interesting possibility for the molecular targets of Shn-2 is the involvement of TRAF2-mediated NF-κB activation. A previous report suggested that there is a physi-

cal association of Shn-3 with TRAF2 (31). Our preliminary results suggest that a physical association of Shn-2 with TRAF2 in 293 T cells can be demonstrated (unpublished data). Thus, Shn proteins may bind to TRAF2 and inhibit the TNFR-induced NF-κB activation and nuclear translocation in T cells. However, this appeared to be unlikely because no obvious difference in the protein expression of p50 and p65 was observed in the cytosol or nucleus before or after anti-TCR stimulation between Shn-2+/+ and Shn-2−/− T cells (Fig. 4 C). Lieberson et al. (37) have reported that Th2 cell responses are enhanced in dominant-negative TRAF2 Tg CD4 T cells. This result would appear to be contradictory to the above hypothesis. However, the dominant-negative TRAF2 used in the study by Lieberson et al. inhibits JNK activity efficiently, but it does not affect NF-κB activity very significantly (38). Thus, it is still possible that the Shn-2–TRAF complex is formed in T cells and that it is involved in the control of Th2 cell differentiation by regulating NF-κB activation. A more precise investigation is needed to clarify this issue.

As for the signaling pathways in which Shn-2 is involved, Shn-2 may regulate outcomes of both the TCR- and TNF-dependent pathways if the major function of Shn-2 is mediated by a mechanism proposed above, namely, competition with NF-κB for DNA binding in the nucleus. In this paper, we focused our analysis mostly on T cells where the TNF-dependent signaling pathway is not activated efficiently, and thus, further investigation will be required to address this issue. In addition, we did not observe CD28 costimulation-mediated enhancement of Th2 cell differentiation in *Shn-2*−/− cells (Fig. S4). CD28 costimulation induced NF-κB activation and enhanced GATA3 expression in developing Th2 cells (36). Thus, it is possible that the effect of CD28 costimulation was masked by hyperactivation of NF-κB in *Shn-2*−/− T cells.

It has been established that the expression of GATA3 is crucial for the efficient Th2 cell differentiation (16). GATA3 plays an essential role in chromatin-remodeling processes, such as acetylation of histone H3 and H4 of the Th2 cell cytokine gene loci (36). The activation of STAT6 is most critical for the induction of GATA3 transcription (16, 39). More recently, several regulatory molecules for GATA3 transcription have emerged. One is the NF-κB activation discussed above (30). We reported previously that a polycomb group gene product, mel-18, controls Th2 cell differentiation by regulating GATA3 transcription (40). Shn-2 is another example of a protein that regulates GATA3 transcription and expression in developing Th2 cells. Further investigation of the regulation of GATA3 expression is likely to provide a clearer molecular view of the initiation of Th2 cell differentiation.

Recombinant TGF-β inhibited Th2 cell differentiation of normal and Shn-2–deficient T cells very efficiently (unpublished data). In addition, Smad7 expression was not changed in *Shn-2*–deficient T cells (unpublished data). Thus, Shn-2 may not be involved in the TGF-β–mediated signal-

ing pathway in T cells, at least not in the TGF-β–mediated inhibition of Th2 cell differentiation. However, because mammalian Shn has three orthologues (Shn-1, Shn-2, and Shn-3), it is still possible that Shn-1 and/or Shn-3 could substitute for the function of Shn-2 in *Shn-2*–deficient T cells.

As for the effects of Shn-2 deficiency on Th1 cell differentiation, Shn-2 may not play critical roles in Th1 cell differentiation. No effect was observed in typical Th1 cell–skewed cultures containing excess amounts of IL-12 (Fig. 1 A). However, we observed some enhancement in Th1 cell differentiation when IL-12 is limiting (Fig. 2 B). Also, IFN-γ–producing cells generated under Th2 cell–skewed conditions were increased consistently (Fig. 1 C). Thus, it is still possible that Shn-2 may act as a negative regulator of the generation of IFN-γ–producing cells.

In summary, the results of this study indicate that Shn-2 plays crucial roles in the control of Th2 cell differentiation by regulating the activation of NF-κB and subsequent GATA3 induction in early developing Th2 cells.

MATERIALS AND METHODS

Mice. *Shn-2*–deficient (*Shn-2⁻/⁻*) mice were described previously (25). Animals used in this study were backcrossed to BALB/c more than 12 times and were 6–8 wk old. Anti-OVA–specific TCR-αβ (DO11.10) Tg mice were provided by D. Loh (Washington University School of Medicine, St. Louis, MO; reference 41). *Shn-2⁻/⁻* × DO11.10 Tg mice were used at 10–12 wk of age. STAT6-deficient (*STAT6⁻/⁻*) mice were provided by S. Akira (Osaka University, Osaka, Japan; reference 39). All mice used in this study were maintained under specific pathogen-free conditions. Animal care was in accordance with the guidelines of Chiba University.

Immunofluorescent staining and flow cytometry analysis. In general, 10⁶ cells were incubated on ice for 30 min with the appropriate staining reagents according to a standard method (42). The reagents used in this study were as follows: anti-CD4–PE (RM4-1–PE), anti-CD4–FITC (RM4-1–FITC), anti-CD44–FITC (IM7-FITC), anti-CD44–PE (IM7-PE), anti-CD69–FITC (H1.2F3), anti-CD62L–FITC (MEL-14), anti-CD25–FITC (7D4), anti–IL-4Rα antibody, and anti–γC antibody-PE were purchased from BD Biosciences. Anti-rat Ig-FITC was purchased from CAPPEL. Anti-TCR-β–FITC (H57-FITC), anti-CD3–FITC (2C11-FITC), and anti-CD8–Cy5 were prepared in our laboratory. Flow cytometry analysis was performed on a FACSCalibur (Becton Dickinson), and results were analyzed with CELLQuest software (Becton Dickinson). Intracellular staining of IL-4 and IFN-γ was performed as described previously (11). FITC-conjugated anti–IFN-γ antibody (XMG1.2), APC-conjugated anti–IL-5 antibody, and PE-conjugated anti–IL-4 antibody (11B11; all from BD Biosciences) were used for detection.

Cell purification. Splenic CD4 T cells were purified by using magnetic beads and an Auto-MACS Sorter (Miltenyi Biotec) yielding a purity of >98%. Where indicated, CD4 T cells with naive phenotype (CD44ˡᵒʷ) were isolated from spleens on a FACSVantage cell sorter (Becton Dickinson) yielding a purity of >98% as described previously (11).

Bone marrow DC cultures. A modified method of Inaba et al. (43) and Chen-Woan et al. (44) was used for bone marrow DC cultures. In brief, bone marrow cells depleted of FcR⁺ cells (0.5–1.0 × 10⁶ cells) were cultured in 1 ml medium in the presence of 10 ng/ml GM-CSF. The culture medium was changed every other day by gently swirling the plates, aspirating ~75% of the medium, and adding back fresh medium with cytokines. On day 6, the cells were harvested and then CD11c⁺ cells (immature DCs) were purified using anti-CD11c mAb-conjugated micro beads and a MACS

LS column (Miltenyi Biotec). The purified immature CD11c⁺ DCs were cultured for an additional 2 d with 10 ng/ml GM-CSF and 1 μg/ml LPS to allow further maturation and were used as mature DCs.

Proliferation assay. 2 × 10⁵ splenic CD4 T cells were stimulated in 200-μl cultures for 40 h with immobilized anti–TCR-β mAb (H57-597) and anti-CD3ε mAb (2C11). Immature or mature DCs were pulsed with 1 μM OVA peptide for 2 h at 37°C and then cocultured with CD4 T cells from DO11.10 Tg mice for 72 h. [³H]thymidine (37 kBq/well) was added to the stimulation culture for the last 16 h, and the incorporated radioactivity was measured by using a β plate (40).

ELISA for the measurement of cytokine concentration. The production of IL-2, IL-4, IL-5, IL-13, and IFN-γ was measured by ELISA as described previously (40).

In vitro Th1/Th2 cell differentiation cultures. Naive splenic CD4 T cells were stimulated with 3 μg/ml of immobilized anti–TCR-β mAb (H57-597) in the presence of 30 U/ml IL-2 and 1–100 U/ml IL-4 as described previously (10). Where indicated, naive splenic CD4 T cells were labeled with CFSE (Molecular Probes) using the same procedure as described previously (40). For Th1 cell differentiation, naive splenic CD4 T cells were stimulated with 3 μg/ml of immobilized anti–TCR-β mAb (H57-597) in the presence of 30 U/ml IL-2, IL-12, and anti–IL-4 mAb. 1.5 × 10⁴ sorted DO11.10 Tg CD44ˡᵒʷ CD4 T cells were stimulated with antigenic OVA peptide (Loh15, OVA; 323–339) and 10⁵ irradiated (3,000 rad) normal BALB/c splenocytes. For stimulation with purified DCs, 2 × 10⁵ sorted DO11.10 Tg CD44ˡᵒʷ CD4 T cells were cocultured with 2 × 10⁴ OVA-pulsed immature or mature DCs. Appropriate cytokines and anti-cytokine antibodies were added in Th1/Th2 cell differentiation cultures as described previously (11). In typical DO11.10 Tg T cell cultures, Th2 cell–skewed (IL-4 with anti–IL-12 mAb and anti–IFN-γ mAb), Th1 cell–skewed (IL-12 with anti–IL-4 mAb), and nonskewed (IL-2 with anti–IL-4 mAb, anti–IL-12 mAb, and anti–IFN-γ mAb) conditions were used.

Immunoblotting. The Immunoblotting for the detection of GATA3, tubulin-α, NFAT1, and NFAT2 was performed as described previously (45). For NF-κB detection, anti-p65 (F-6), anti-p50 (E-10), and anti–histone H1 (AE-4, all from Santa Cruz Biotechnology, Inc.) antibodies were used.

EMSA. EMSAs were performed using Gel Shift Assay Systems (Promega) according to the manufacturer's instructions. In brief, nuclear extracts were incubated at 4°C with ³²P-labeled double-stranded oligo (NF-κB oligo: AGTTGAGGGGACTTTCCCAGGC. AP-1 oligo: CGCTTGATGAGT-CAGCCGGAA, CREB oligo: AGAGATTGCCTGACGTCAGAGAG-CTAG, IL-4 NFAT: oligo; and GTAATAAAATTTTCCAATGTAAA) in DNA binding buffer (Promega). For supershift assays, nuclear extracts were incubated with anti-p50 (C-19; Santa Cruz Biotechnology, Inc.) or anti-p65 (F-6; Santa Cruz Biotechnology, Inc.) antibody at 4°C for 60 min and then incubated with ³²P-labeled NF-κB double-stranded oligo at 4°C. Electrophoresis was performed on a 4% native polyacrylamide gel (0.5× TBE; acrylamide/bisacrylamide, 29:1), and the radioactivity was visualized by autoradiography.

Pull-down assay. A detailed protocol was described elsewhere (46). In brief, 293 T cells were transfected with 1.0 μg pAct or pAct-Flag-hShn-2, and 2 d later, the transfected cells were lysed for immunoblotting with anti-Flag mAb (M2; Sigma-Aldrich). Cell lysates were incubated with biotinylated oligonucleotides of NF-κB (AGTTGAGGGGACTTTCCCAGGC) and AP-1 (CGCTTGATGAGTCAGCCGGAA). The bound protein were eluted and separated on an SDS polyacrylamide gel and then subjected to immunoblot analysis using specific antibodies (anti-Flag Tag; M2; Sigma-Aldrich). For the competition assay shown in Fig. 6 B, 293 T cells were transfected with pAct-Flag-hShn-2 or pCMX-p50, and their cell extracts were mixed in certain ratios and then the mixed extracts were incubated

406

with NF-κB oligonucleotides as described above. pCMX-p50 was provided by J. Inoue (University of Tokyo, Tokyo, Japan). Anti-Flag Tag (M2; Sigma-Aldrich) mAb and anti-p50 (E-10; Santa Cruz Biotechnology, Inc.) mAb were used for detection.

Transfection and luciferase assays. 293 T cells were transfected with 5× NF-κB luciferase reporter plasmid together with pAct vector or pAct-Flag-hShn-2 vector and pRL-TK as normalization control. Transfected cells were stimulated with or without 50 ng/ml PMA and 500 nM ionomycin or 10 ng/ml TNF-α for 12 h before luciferase assays (Promega).

PCR analysis. Total RNA was isolated from cultured cells using the TRIzol reagent. Reverse transcription was performed with Superscript II RT (Invitrogen). Threefold serial dilutions of template cDNA were performed. The PCR reaction was performed as described previously (46). The primers used are as follows: β actin forward, GAGAGGGAAATCGTGCGTGA-3'; β actin reverse, 5'-ACATCTGCTGGAAGGTGGAC; GATA3 forward, gAAggCATCCAgACCCgAAAC-3'; GATA3 reverse, 5'-ACCCATgg-CggTgACCATgC; Shn-2 forward, ggAAAgAgggAAAggAgAgATTCA-CggAgAT-3'; and Shn-2 reverse, 5'-ATCTgAgTgTCATCACAAgAgT-CACTgggT.

For quantitative PCR assay, first-strand cDNA was synthesized using random primers and Superscript II RT (Invitrogen). Samples were then subjected to real-time PCR analysis on an ABI PRISM 7000 Sequence Detection System (Applied Biosystems) under standard conditions. The primers and TaqMan probes for the detection of p50, p65, T-bet, and 18S were purchased from Applied Biosystems. p50, p65, and T-bet expression were normalized using the 18S signal.

Online supplemental material. Fig. S1 shows the phenotypic feature of splenic CD4 T cells from Shn-2$^{-/-}$ mice. (A) The yields of thymocytes and splenocytes are shown in boxed numbers. (B) Each histogram depicts the expression of the indicated marker antigens on electronically gated splenic CD4 T cells. Background staining is shown as hatched areas. (C) The histogram shows the percentages of indicated Vβ cells among splenic CD4 T cells. Fig. S2 shows the proliferative responses and Erk phosphorylation status after TCR stimulation. Arbitrary densitometric units are shown under each band in B. Fig. S3 shows the expression of Shn-2 mRNA in developing Th1 and Th2 cells. The mRNA levels were determined by RT-PCR with threefold serial dilutions of template cDNA. Fig. S4 shows the effects of CD28 stimulation on Th2 cell differentiation. Gel shift assay for AP-1, CREB, or IL-4 NFAT are shown in Fig. S5. Figs. S1–S5 are available at http://www.jem.org/cgi/content/full/jem.20040733/DC1.

REFERENCES

1. Mosmann, T.R., and R.L. Coffman. 1989. TH1 and TH2 cells: different patterns of lymphokine secretion lead to different functional properties. Annu. Rev. Immunol. 7:145–173.

2. Seder, R.A., and W.E. Paul. 1994. Acquisition of lymphokine-producing phenotype by CD4$^+$ T cells. Annu. Rev. Immunol. 12:635–673.

3. Reiner, S.L., and R.M. Locksley. 1995. The regulation of immunity to Leishmania major. Annu. Rev. Immunol. 13:151–177.

4. Abbas, A.K., K.M. Murphy, and A. Sher. 1996. Functional diversity of helper T lymphocytes. Nature. 383:787–793.

5. Constant, S.L., and K. Bottomly. 1997. Induction of Th1 and Th2 CD4+ T cell responses: the alternative approaches. Annu. Rev. Immunol. 15:297–322.

6. Nelms, K., A.D. Keegan, J. Zamorano, J.J. Ryan, and W.E. Paul. 1999. The IL-4 receptor: signaling mechanisms and biologic functions. Annu. Rev. Immunol. 17:701–738.

7. O'Garra, A. 1998. Cytokines induce the development of functionally heterogeneous T helper cell subsets. Immunity. 8:275–283.

8. Murphy, K.M., W. Ouyang, J.D. Farrar, J. Yang, S. Ranganath, H. Asnagli, M. Afkarian, and T.L. Murphy. 2000. Signaling and transcription in T helper development. Annu. Rev. Immunol. 18:451–494.

9. Yamashita, M., K. Hashimoto, M. Kimura, M. Kubo, T. Tada, and T. Nakayama. 1998. Requirement for p56^{lck} tyrosine kinase activation in Th subset differentiation. Int. Immunol. 10:577–591.

10. Yamashita, M., M. Katsumata, M. Iwashima, M. Kimura, C. Shimizu, T. Kamata, T. Shin, N. Seki, S. Suzuki, M. Taniguchi, and T. Nakayama. 2000. T cell receptor–induced calcineurin activation regulates T helper type 2 cell development by modifying the interleukin 4 receptor signaling complex. J. Exp. Med. 191:1869–1879.

11. Yamashita, M., M. Kimura, M. Kubo, C. Shimizu, T. Tada, R.M. Perlmutter, and T. Nakayama. 1999. T cell antigen receptor–mediated activation of the Ras/mitogen–activated protein kinase pathway controls interleukin 4 receptor function and type-2 helper T cell differentiation. Proc. Natl. Acad. Sci. USA. 96:1024–1029.

12. Kamata, T., M. Yamashita, M. Kimura, K. Murata, M. Inami, C. Shimizu, K. Sugaya, C.R. Wang, M. Taniguchi, and T. Nakayama. 2003. src homology 2 domain-containing tyrosine phosphatase SHP-1 controls the development of allergic airway inflammation. J. Clin. Invest. 111:109–119.

13. Zhang, D.H., L. Cohn, P. Ray, K. Bottomly, and A. Ray. 1997. Transcription factor GATA-3 is differentially expressed in murine Th1 and Th2 cells and controls Th2-specific expression of the interleukin-5 gene. J. Biol. Chem. 272:21597–21603.

14. Zheng, W., and R.A. Flavell. 1997. The transcription factor GATA-3 is necessary and sufficient for Th2 cytokine gene expression in CD4 T cells. Cell. 89:587–596.

15. Ouyang, W., S.H. Ranganath, K. Weindel, D. Bhattacharya, T.L. Murphy, W.C. Sha, and K.M. Murphy. 1998. Inhibition of Th1 development mediated by GATA-3 through an IL-4-independent mechanism. Immunity. 9:745–755.

16. Lee, H.J., N. Takemoto, H. Kurata, Y. Kamogawa, S. Miyatake, A. O'Garra, and N. Arai. 2000. GATA-3 induces T helper cell type 2 (Th2) cytokine expression and chromatin remodeling in committed Th1 cells. J. Exp. Med. 192:105–115.

17. Szabo, S.J., S.T. Kim, G.L. Costa, X. Zhang, C.G. Fathman, and L.H. Glimcher. 2000. A novel transcription factor, T-bet, directs Th1 lineage commitment. Cell. 100:655–669.

18. Affolter, M., T. Marty, M.A. Vigano, and A. Jazwinska. 2001. Nuclear interpretation of Dpp signaling in Drosophila. EMBO J. 20:3298–3305.

19. Arora, K., H. Dai, S.G. Kazuko, J. Jamal, M.B. O'Connor, A. Letsou, and R. Warrior. 1995. The Drosophila schnurri gene acts in the Dpp/TGFβ signaling pathway and encodes a transcription factor homologous to the human MBP family. Cell. 81:781–790.

20. Staehling-Hampton, K., A.S. Laughon, and F.M. Hoffmann. 1995. A Drosophila protein related to the human zinc finger transcription factor PRDII/MBPI/HIV-EP1 is required for dpp signaling. Development. 121:3393–3403.

21. Kingsley, D.M. 1994. The TGF-β superfamily: new members, new receptors, and new genetic tests of function in different organisms. Genes Dev. 8:133–146.

22. Makino, R., K. Akiyama, J. Yasuda, S. Mashiyama, S. Honda, T. Sekiya, and K. Hayashi. 1994. Cloning and characterization of a c-myc intron binding protein (MIBP1). Nucleic Acids Res. 22:5679–5685.

23. Ron, D., A.R. Brasier, and J.F. Habener. 1991. Angiotensinogen gene-inducible enhancer-binding protein 1, a member of a new family of large nuclear proteins that recognize nuclear factor kappa B-binding sites through a zinc finger motif. *Mol. Cell. Biol.* 11:2887–2895.

24. Campbell, D.B., and P. Levitt. 2003. Regionally restricted expression of the transcription factor c-myc intron 1 binding protein during brain development. *J. Comp. Neurol.* 467:581–592.

25. Takagi, T., J. Harada, and S. Ishii. 2001. Murine Schnurri-2 is required for positive selection of thymocytes. *Nat. Immunol.* 2:1048–1053.

26. Allen, C.E., N. Muthusamy, S.E. Weisbrode, J.W. Hong, and L.C. Wu. 2002. Developmental anomalies and neoplasia in animals and cells deficient in the large zinc finger protein KRC. *Genes Chromosomes Cancer.* 35:287–298.

27. Barnes, P.J., and M. Karin. 1997. Nuclear factor-κB: a pivotal transcription factor in chronic inflammatory diseases. *N. Engl. J. Med.* 336:1066–1071.

28. Yang, L., L. Cohn, D.H. Zhang, R. Homer, A. Ray, and P. Ray. 1998. Essential role of nuclear factor κB in the induction of eosinophilia in allergic airway inflammation. *J. Exp. Med.* 188:1739–1750.

29. Donovan, C.E., D.A. Mark, H.Z. He, H.C. Liou, L. Kobzik, Y. Wang, G.T. De Sanctis, D.L. Perkins, and P.W. Finn. 1999. NF-κB/Rel transcription factors: c-Rel promotes airway hyperresponsiveness and allergic pulmonary inflammation. *J. Immunol.* 163:6827–6833.

30. Das, J., C.H. Chen, L. Yang, L. Cohn, P. Ray, and A. Ray. 2001. A critical role for NF-κB in GATA3 expression and TH2 differentiation in allergic airway inflammation. *Nat. Immunol.* 2:45–50.

31. Oukka, M., S.T. Kim, G. Lugo, J. Sun, L.C. Wu, and L.H. Glimcher. 2002. A mammalian homolog of *Drosophila schnurri*, KRC, regulates TNF receptor-driven responses and interacts with TRAF2. *Mol. Cell.* 9:121–131.

32. Bachmeyer, C., C.H. Mak, C.Y. Yu, and L.C. Wu. 1999. Regulation by phosphorylation of the zinc finger protein KRC that binds the κB motif and V(D)J recombination signal sequences. *Nucleic Acids Res.* 27:643–648.

33. Hong, J.W., C.E. Allen, and L.C. Wu. 2003. Inhibition of NF-κB by ZAS3, a zinc-finger protein that also binds to the κB motif. *Proc. Natl. Acad. Sci. USA.* 100:12301–12306.

34. Bird, J.J., D.R. Brown, A.C. Mullen, N.H. Moskowitz, M.A. Mahowald, J.R. Sider, T.F. Gajewski, C.R. Wang, and S.L. Reiner. 1998. Helper T cell differentiation is controlled by the cell cycle. *Immunity.* 9:229–237.

35. Kubo, M., M. Yamashita, R. Abe, T. Tada, K. Okumura, J.T. Ransom, and T. Nakayama. 1999. CD28 costimulation accelerates IL-4 receptor sensitivity and IL-4-mediated Th2 differentiation. *J. Immunol.* 163:2432–2442.

36. Inami, M., M. Yamashita, Y. Tenda, A. Hasegawa, M. Kimura, K. Hashimoto, N. Seki, M. Taniguchi, and T. Nakayama. 2004. CD28 costimulation controls histone hyperacetylation of the interleukin 5 gene locus in developing th2 cells. *J. Biol. Chem.* 279:23123–23133.

37. Lieberson, R., K.A. Mowen, K.D. McBride, V. Leautaud, X. Zhang, W.K. Suh, L. Wu, and L.H. Glimcher. 2001. Tumor necrosis factor receptor–associated factor (TRAF)2 represses the T helper cell type 2 response through interaction with NFAT-interacting protein (NIP45). *J. Exp. Med.* 194:89–98.

38. Lee, S.Y., A. Reichlin, A. Santana, K.A. Sokol, M.C. Nussenzweig, and Y. Choi. 1997. TRAF2 is essential for JNK but not NF-κB activation and regulates lymphocyte proliferation and survival. *Immunity.* 7:703–713.

39. Takeda, K., T. Tanaka, W. Shi, M. Matsumoto, M. Minami, S. Kashiwamura, K. Nakanishi, N. Yoshida, T. Kishimoto, and S. Akira. 1996. Essential role of Stat6 in IL-4 signalling. *Nature.* 380:627–630.

40. Kimura, M., Y. Koseki, M. Yamashita, N. Watanabe, C. Shimizu, T. Katsumoto, T. Kitamura, M. Taniguchi, H. Koseki, and T. Nakayama. 2001. Regulation of Th2 cell differentiation by mel-18, a mammalian polycomb group gene. *Immunity.* 15:275–287.

41. Murphy, K.M., A.B. Heimberger, and D.Y. Loh. 1990. Induction by antigen of intrathymic apoptosis of CD4⁺CD8⁺TCR^lo thymocytes *in vivo. Science.* 250:1720–1723.

42. Nakayama, T., C.H. June, T.I. Munitz, M. Sheard, S.A. McCarthy, S.O. Sharrow, L.E. Samelson, and A. Singer. 1990. Inhibition of T cell receptor expression and function in immature CD4⁺CD8⁺ cells by CD4. *Science.* 249:1558–1561.

43. Inaba, K., M. Inaba, N. Romani, H. Aya, M. Deguchi, S. Ikehara, S. Muramatsu, and R.M. Steinman. 1992. Generation of large numbers of dendritic cells from mouse bone marrow cultures supplemented with granulocyte/macrophage colony-stimulating factor. *J. Exp. Med.* 176:1693–1702.

44. Chen-Woan, M., C.P. Delaney, V. Fournier, Y. Wakizaka, N. Murase, J. Fung, T.E. Starzl, and A.J. Demetris. 1995. A new protocol for the propagation of dendritic cells from rat bone marrow using recombinant GM-CSF, and their quantification using the mAb OX-62. *J. Immunol. Methods.* 178:157–171.

45. Omori, M., M. Yamashita, M. Inami, M. Ukai-Tadenuma, M. Kimura, Y. Nigo, H. Hosokawa, A. Hasegawa, M. Taniguchi, and T. Nakayama. 2003. CD8 T cell-specific downregulation of histone hyperacetylation and gene activation of the IL-4 gene locus by ROG, repressor of GATA. *Immunity.* 19:281–294.

46. Yamashita, M., M. Ukai-Tadenuma, M. Kimura, M. Omori, M. Inami, M. Taniguchi, and T. Nakayama. 2002. Identification of a conserved GATA3 response element upstream proximal from the interleukin-13 gene locus. *J. Biol. Chem.* 277:42399–42408.

— 96 —

Differentiation of NK1 and NK2 Cells

Motoko Y. Kimura & Toshinori Nakayama*

Department of Immunology, Graduate School of Medicine, Chiba University, 1-8-1 Inohana, Chuo-ku, Chiba 260-8670, Japan

* Address all correspondence to Toshinori Nakayama, MD, PhD, Department of Immunology (H3), Graduate School of Medicine, Chiba University, 1-8-1 Inohana, Chuo-ku, Chiba 260-8670, Japan; Tel.: +81-43-226-2200, Fax: +81-43-227-1498, email: tnakayama@faculty.chiba-u.jp

ABSTRACT: Natural killer type-1 (NK1)/NK2 terminology was proposed as an analogy to T helper type-1 (Th1)/Th2 subsets of CD4 T cells. In addition to well recognized IFN-γ–producing NK1 cells, recent accumulating evidence suggests the presence and the regulatory function of NK2 cells, which produce type-2 cytokines, such as IL-5 and IL-13. Most studies on the production of cytokines by NK1/NK2 subsets have been performed in the human system. Recently, a mouse *in vitro* NK1/NK2 cell differentiation system was established. A linear "2–0–1" model has been proposed for the differentiation of NK1/NK2 cell subsets, but the branching NK1/NK2 cell differentiation model, comparable to Th1/Th2 cell differentiation, remains a likely explanation. In this review, we summarize the evidence indicating the unique features of NK1/NK2 cells and discuss the above two NK cell differentiation models. In addition, we point to interesting similarities in the expression of transcription factors that regulate cytokine production in NK cells and CD8 T cells.

KEY WORDS: type-2 cytokine, linear "2–0–1" differentiation model, branching NK1/NK2 differentiation model, GATA3, ROG, immune regulation

I. INTRODUCTION

Natural killer type-1 (NK1)/NK2 terminology was proposed as an analogy to T helper type-1 (Th1)/Th2 subsets of CD4 T cells.[1] Th1 cells produce IFN-γ to control cell-mediated immunity against intracellular pathogens. Th2 cells produce IL-4, IL-5, and IL-13 and are involved in humoral immunity and allergic reactions.[2,3] It has been well documented that NK cells produce IFN-γ and play crucial roles during infection and in antitumor immunity. There are excellent recent reviews.[4–7] However, there is accumulating evidence to indicate that some human NK cells produce type-2 cytokines as well. Recently, we established an *in vitro* mouse NK1/NK2 cell differentiation system and reported that *in vitro* differentiated mouse NK2 cells produce IL-13 and IL-5, but not IL-4 or IFN-γ.[8] Although the roles

for NK2 cells in host-defense immune responses remain undetermined, the unique cytokine production profile of NK2 cells suggests that these cells may play important roles in specific immune responses, including the regulation of allergic or autoimmune diseases. In this review, we summarize the current understanding of the features of NK1/NK2 cells and discuss two proposed NK1/NK2 cell differentiation models.

II. EVIDENCE FOR THE PRESENCE OF NK1/NK2 CELL SUBSETS

It has been well documented that activated NK cells produce IFN-γ, TNF-α, and GM-CSF.[9–11] From the late 1990s, various investigators have reported evidence indicating the presence of type-2 cytokine-producing NK cell subsets, particularly

361

in human systems (Table 1). Proliferating human NK cells were shown to produce IL-5, and the production of IL-5 was augmented by IL-4 and inhibited by IL-12 and IL-10.[12] Human NK cells cultured with IL-12 produce IL-10 and IFN-γ, whereas those cultured with IL-4 produce IL-5 and IL-13.[1] Similarly, human NK cells stimulated with IL-12 produce increased levels of IFN-γ and decreased levels of IL-4, whereas IL-4 stimulation inhibits IFN-γ and increases the level of IL-13.[13] Intracellular staining analysis revealed that about 2% of human peripheral NK cells produce IL-13 in response to IL-2.[14] These findings are reminiscent of the cytokine-mediated counter-regulation of Th1/Th2 subsets. In addition, separate studies focused on NK cell ontogeny identified the presence of IL-5/IL-13–secreting NK cells, which can be defined by their CD161 expression.[15] Single cell analysis of adult and neonatal human NK cells revealed CD161+ IL-13–producing NK cells to be a nonoverlapping population with IFN-γ-producing NK cells expressing CD56.[16] The size of the IL-13+ NK cell subset was expanded by IL-4, and this expansion was inhibited by IL-12. Also, the size of the IFN-γ-producing subset was down-regulated by IL-4 and IL-13. Thus, similar to the generation of Th1/Th2 cells, cytokines in the local microenvironment appear to control the development of distinct cytokine-producing NK cell subsets. Taken together, it now seems reasonable to accept type-2 cytokine-producing NK2 cells as a distinct subset within NK cells.

III. UNIQUE CYTOKINE PRODUCTION PROFILES IN NK1/NK2 CELLS

It is recognized that NK2 cells produce significant amounts of IL-5 and IL-13 but little IL-4 in both human[1,12,14] and mouse.[8] This production profile is different from that of Th2 cells.[2,3] From studies with mouse NK1/NK2 cells, we proposed a possible molecular mechanism to explain the unique production profiles of type-2 cytokines in NK2 cells.[8] *In vitro* mouse differentiated NK2 cells produce IL-5 and IL-13, but the levels on a per-cell basis are 20 times lower than those of *in vitro* differentiated Th2 cells. In addition, no detectable IL-4 is produced. In developing NK2 cells, the expression levels of GATA3 are significantly

higher than in fresh NK, NK0, or NK1 cells but significantly lower than in Th2 cells. Other GATA family members, such as GATA1 and GATA2, are not expressed in NK cells. Th2 cell differentiation is known to be highly dependent on the expression levels of GATA3.[17-19] GATA3 is required for chromatin remodeling of the IL-4/IL-13 gene loci in Th2 cells and Tc2 cells[20,21] and the IL-5 gene locus in Th2 cells.[22] In fact, one of the indicators of chromatin remodeling, the levels of histone H3/K9 acetylation of the IL-4, IL-13, and IL-5 gene loci, is impaired in *in vitro* differentiated NK2 cells.[8] In addition, GATA3 is known to be very important for the transcription of the IL-13 and IL-5 genes.[17,23,24] Thus, we believe that the unique type-2 cytokine production profiles of NK2 cells could be associated with the low expression level of GATA3 in developing NK2 cells. However, there should be another factor that regulates the selective production of IL-5 and IL-13 among the three type-2 cytokines (IL-4, IL-13, and IL-5) in NK2 cells.

A POZ/BTB-domain–containing zinc finger transcriptional repressor, repressor of GATA (ROG), has been reported to inhibit GATA3 function[25] and to play crucial roles in cytokine expression and chromatin remodeling in developing type-2 cytokine-producing CD8 T (Tc2) cells.[21] The expression levels of ROG in activated CD8 T cells are ten times higher than those in CD4 T cells. ROG is highly expressed in NK0, NK1, and NK2 cells, with expression levels much higher than those in Th2 cells and equivalent to those in Tc1 and Tc2 cells.[8] Thus, the lack of detectable IL-4 production in NK2 cells may be due to both the low-level induction of GATA3 and the high-level expression of ROG. This is reminiscent of the limited IL-4 production and substantial IL-13 and IL-5 production in CD8+ Tc2 cells.[21]

In *in vitro* differentiated mouse NK1 and NK2 cells, STAT6 has been found to be required for the differentiation of NK2 cells.[8] IL-5/IL-13–producing NK2 cells are not generated from STAT6-deficient mouse splenic NK cells, whereas IFN-γ–producing NK1 cells are generated normally. Thus, STAT6 and GATA3 appear to play important roles in the differentiation of NK2 cells.[8] In fact, IL-4 and IL-13 induce STAT6 activation and STAT6-containing protein DNA complexes in NK cells.[26] As for GATA3, roles in